

REPUBLIC OF AZERBAIJAN

On the rights of the manuscript

ABSTRACT

of the dissertation for the degree of Doctor of Science

THE EFFECT OF NEUTRON FLUX ON THE RADIATION TRANSFORMATIONS AND ELECTRONIC PROCESSES IN THE NANOCRYSTALLINE 3C-SiC

Speciality: 2225.01 Radiation materials science

Field of science: Physics

Applicant: **Elchin Mammadali oglu Huseynov**

Baku – 2021

The work was performed at Institute of Radiation Problems of Azerbaijan National Academy of Sciences

Official opponents:

Doctor of physical and mathematical sciences, professor
Ogtay Bahadir oglu Tagiyev


Doctor of physical sciences, professor
Adil Polad oglu Abdullayev

Doctor of physical sciences, professor
Mirteymur Mirkazim oglu Mirabutalybov

Doctor of physical sciences, associate professor
Nushabe Nubarek gizi Hacıyeva

Dissertation council BED 1.21 of Supreme Attestation Commission under the President of the Republic of Azerbaijan operating at Institute of Radiation Problems of Azerbaijan National Academy of Sciences


Chairman of the Dissertation Council:


Correspondent member of ANAS
Doctor of physical and mathematical sciences, professor
Ogtay Abil oglu Samadov

Scientific secretary of the Dissertation council:


Doctor of philosophy on physics
Muslum Ahmad oglu Mammadov

Chairman of the scientific seminar:


Doctor of physical sciences,
associate professor
Matanat Ahmad gizi Mehrabova

GENERAL DESCRIPTION OF WORK

The relevance of the topic. Recently obtaining new materials or modification of existing materials in micro- and nanoelectronics is the focus of world researchers. SiC is practically attractive material in the electronics due to the physical and chemical properties. High-temperature stability, perfect structure, mechanical resistivity, low oxidation capacity increases application potential of SiC. The combinations of amazing mechanical and functional properties of SiC are the basis of the wide application as a semiconductor in modern micro- and nanoelectronics. The Si and C atoms in SiC are combined with different modifications and it's lead to the formation of more than 200 polytypes. The main reason for excellent mechanical and chemical stability is a short distance between the atoms in most of the polytypes. Moreover, from the semiconductor point of view silicon carbide has wide band-gap (2,4eV – 3,2eV) depending on the polytypes. SiC can form as amorphous, polycrystal and single crystal in various polytypes. The most commonly used silicon carbide polytypes are cubic (3C-SiC) and hexagonal (4H-SiC and 6H-SiC) modified compounds. Nanocrystalline 3C-SiC has wide application possibilities in nanoelectronics devices due to the multifunctional properties. For this reason, the nano 3C-SiC (also known as β -SiC) particles with cubic modifications were used in all experiments in the present study.

The materials in nanoscale have a very large specific surface area (SSA), therefore have a different physical properties. Silicon carbide has unique functional and new distinct physical properties like other materials in nanoscale. The large specific surface area in nanomaterials can cause sharp differences at physical and especially electrophysical processes on the surface.

Over the past few years, one of the most actual problems in the world is the control or modification of physical properties of materials in nanoscale. Although different approaches have been made by researchers in this direction, possible changes in silicon carbide nanocrystals under the neutron flux have not been studied. In this approach, the content of the presented dissertation is the

doping of nanocrystalline 3C-SiC particles by neutron flux. So, the nanomaterials are very small and sensitive and therefore neutron flux is a perfect method for doping. Doping of materials by neutron flux are considered to be the most accurate and sensitive method in the world. One of the main purposes in the work is managing and forming possible changes in physical properties of nanocrystalline 3C-SiC particles by neutron flux. Neutron-modified nanocrystalline 3C-SiC particles may produce a new and different type of dopants. Naturally, the silicon in the nanocrystalline 3C-SiC particles are consist of 92.23% ^{28}Si , 4.67% ^{29}Si and 3.1% ^{30}Si isotopes. All three silicon isotopes are stable and do not undergo radioactive transformation. However, ^{30}Si isotope captures one neutron and modifies to ^{31}Si radioactive isotope during the neutron irradiation. The ^{31}Si isotope is an active isotope with a half-life of 157.36 min. As a result of the β decay, the ^{31}Si isotope is turned to the ^{31}P and this isotope is n-type dopant in the 3C-SiC nanomaterial.

An increasing or decreasing of the concentration of ^{31}P isotope cause changes in the physical properties of nanocrystalline 3C-SiC particles proportionally to neutron irradiation duration. It is important to note that, the second nuclear reaction may occur at a very low propability. In that case, ^{31}P isotope can be modified to ^{32}P isotope by capturing one neutron. The ^{32}P is also β active isotope with 14 days half-life and it's transformed to ^{32}S isotope. However the probability of ^{32}S isotope formation is very low and depends directly on the concentration of the ^{31}P isotope. Nanocrystalline 3C-SiC particles can also be doped by ^{14}N isotopes with an analogical approach. However, this process is somewhat complex and has low efficiency. For this reason, only ^{31}P isotope doped of nanocrystalline 3C-SiC particles and the processes of the controlling of physical properties were studied in the presented work.

All experiments in the dissertation were carried out at the Institute of Radiation Problems of ANAS and in the various centers and laboratories of the Jozef Stefan Institute in Slovenia. As a neutron source, TRIGA Mark II light water type nuclear research reactor was used at "Reactor Center" of the Jozef Stefan Institute.

The main purpose of the dissertation - is to modificate the

physical properties of 3C-SiC nanocrystals under the neutron irradiation, to investigate changes with different spectroscopic approaches, to study possible neutron transformations within nanomaterials, to doping the nanocrystals by neutron transmutation method and to investigate the properties of the doped nanocrystals.

The following tasks were set to achieve this goal:

- Study of possible neutron transformations and the new isotopes by k_0 -INAA method in nanocrystalline 3C-SiC particles under the neutron irradiation.
- Study of neutron irradiation on the structure of 3C-SiC nanocrystals by SAED, EDP and X-ray method
- Analysis of nanocrystalline 3C-SiC particle size and surface morphology using HRTEM, TEM, FESEM and SEM methods
- General modeling of interaction of 3C-SiC nanocrystals with neutron flux and study of effective neutron energy
- Investigation of radiation-induced conductivity (RIC) on 3C-SiC nanocrystals
- Study of the effect of neutrons transformations on the electrical conductivity, as well as temperature and frequency dependence of 3C-SiC nanocrystals
- Investigation of defects formation and the concentration of the formed new dopants by EPR method on nanocrystalline 3C-SiC particles
- Investigation of dielectric properties of 3C-SiC nanocrystals as a function of neutron irradiation
- Investigation of neutron doping by impedance spectroscopy and reciprocal analysis of impedance spectra of 3C-SiC nanocrystals

Research object – is cubic modifications nanocrystalline silicon carbide (3C-SiC) particles with 120 m²/g specific surface area, 18nm particles size and 0.03g/cm³ (3.216 g/cm³ true density) density.

Investigation methods: Several investigation methods were used with different approaches to achieve the goal in this study. TRIGA MARK II type nuclear research reactor were used as the neutron source in the work and standard methods were used during the neutron irradiation. The method of k_0 -INAA was used to

determination of possible radioactive transmutations and new isotopes in the nanocrystalline 3C-SiC particles. Computer modelling was performed for interaction between 3C-SiC nanocrystals with neutrons before neutron irradiation. HRTEM, TEM, FESEM, SAED, EDP and SEM methods were applied to study of structure, radiation defects, other ionization irradiation effects in 3C-SiC nanocrystals. Simultaneously, DSC, DTA, TGA and TG methods were used to investigate the thermal properties of nanomaterial. Moreover, the impedance spectroscopy method was applied to the study of electrical and dielectrical properties of 3C-SiC nanocrystals. The current-voltage (V – A) characterization of 3C-SiC nanocrystals was studied by standard method. The EPR spectroscopy was used to study the defect and paramagnetic centers formed in the SiC nanocrystals.

The scientific novelties of the dissertation are consist of as follows: For the first time in the presented dissertation:

- Neutron transformations were found on 3C-SiC nanocrystals and n - type dopants were obtained by neutron transmutation method within nanocrystalline 3C-SiC particles
- HRTEM, TEM, FESEM and SEM analyzes are shown that nanocrystalline 3C-SiC particles agglomerated maximum 70-80 nm as a result of neutron irradiation.
- After neutron irradiation, there is an approximately 3 nm thick amorphous layer were determined on the surface of nanocrystalline 3C-SiC nanoparticles
- HRTEM analyzes were confirmed nanocrystalline nature of 3C-SiC particles and the formed defects or clusters in nanomaterial were determined by “spots” after neutron irradiation
- The lattice parameters of nanocrystalline 3C-SiC particles were determined by EDP, SAED and X-ray analyzes as (1 1 1), (2 0 0), (2 2 0), (3 1 1), (2 2 2), $a=b=c=4,377565$ and $\alpha=\beta=\gamma=90^0$
- Minimum energies of observed resonance states in absorption spectra of ^{28}Si , ^{29}Si and ^{30}Si isotopes were found by computer modelling as $5 \cdot 10^{-2}$ MeV, 10^{-2} MeV and 10^{-3} MeV, respectively
- RIC conductivity were determined on 3C-SiC nanocrystals after neutron irradiation

- It was shown that the electrical conductivity are increase up to 7.5×10^{-4} S/m or 5.5 times on 3C-SiC nanocrystals consequence of n-type doping by neutrons
- Metal-semiconductor transition was found from impedance spectroscopy of 3C-SiC nanocrystals at $T_{MS} = 250K, 325K$ and $370K$ temperatures according to the values of $0.1MHz, 1MHz$ and $2.5MHz$ frequencies
- It was shown the resistance of 3C-SiC nanoparticles are reduced from $4 M\Omega$ to $1 M\Omega$
- It was shown that the total number of paramagnetic centers in different values of the g-factor are increased from 1.5×10^{20} center/g to 2.7×10^{20} center/g (approximately 2 times) after neutron irradiation
- The concentration of the center of free electrons or the concentration of n-type dopants were determined approximately 0.7×10^{16} as a result of the increase of irradiation time by neutron flux of 3C-SiC nanocrystals
- The 3C-SiC nanocrystals show the decrease in Debay temperature from $1200K$ to $800K$ as typical for nanomaterials
- Specific heat capacity, heat flux, oxidation rate, activation energy, Gibbs energy, enthalpy and entropy of nanocrystalline 3C-SiC particles found out before and after neutron irradiation.

The possibility of practical application: According to the main scientific results obtained in the dissertation, nanocrystalline 3C-SiC particles can be applied in nanoelectronics as a perfect material in various environments, with n-type doping, without affecting the crystal structure with neutron flux. Simultaneously, it was shown that some physical properties of 3C-SiC nanocrystals can be controlled with modification by neutron flux, and this increase application perspectives of these materials in the electronics. In general approach, managing the physical properties of nanomaterials is a very complex and important issue. Conducted experiments have shown that the concentration of dopants in nanocrystalline 3C-SiC particles can be controlled by the neutrons. The changes in the concentration of newly formed dopant elements directly influence changes in the physical properties of nanomaterials. The dissertation was carried out in multidisciplinary frameworks in combination with

radiation material science, nuclear physics, nanostructures and semiconductor physics. In this study, a new type of nanocrystalline 3C-SiC material with different properties was modified by neutron flux. Its possible to extend useful work ratios or exploitation time of nanoparts of the microelectronics devices or nanoelectronics devices by obtained new material. Simultaneously, obtained nanomaterials with new and perfect properties acquired are more economically viable. Moreover, managing the physical properties of nanomaterials will allow the substitution of other alternative materials with these materials. In general approach, the new 3C-SiC nanomaterials obtained as a result of neutron transmutation method have a wide range of application potential in microelectronics, nanoelectronics, microelectromechanical systems (MEMS), nanoelectromechanical systems (NEMS) and ionizing environments (satellite (space) technologies, nuclear technologies etc).

Main provisions for the defense:

- Possibility neutron transmutations in nanocrystalline 3C-SiC particles
- Changes in structure of 3C-SiC nanocrystals formed by neutron flux
- Effective neutron energy during interaction with 3C-SiC nanocrystals
- Surface morphology, nanocrystalline nature of materials, amorphous and agglomeration rate of the nanocrystalline 3C-SiC particles
- n-type doping of 3C-SiC nanocrystals by neutron flux at various concentrations
- Radiation-induced conductivity (RIC) in 3C-SiC nanocrystals
- Neutron transmutation effects on electrical and dielectrical properties of 3C-SiC nanocrystals.
- Defects formation processes in nanocrystalline 3C-SiC particles under the neutron irradiation
- Relaxation time and metal-semiconductor transition in 3C-SiC nanocrystals
- Neutron irradiation effects on thermal parameters of 3C-SiC nanocrystals

Approbation of the dissertation: The main results of dissertation work were discussed at several national and international conferences and seminars.

- XXVII International Materials Research Congress, F2. Advances in functional semiconducting materials - IMRC 2018, 2879-2880, August 19-24, 2018, Cancun, Mexico
- II international scientific conference of young researcher: dedicated to the 91rd anniversary of the national leader of Azerbaijan, Haydar Aliyev, 67-69, 27-28 April 2018,, Baku, Azerbaijan
- DPG-Frühjahrstagung und EPS-CMD27, Technische Universität Berlin, Deutsche Physikalische Gesellschaft e.V., 137/188, O 81.17, 11 - 16 March 2018, Berlin, Germany
- 27th International Conference Nuclear Energy for New Europe, 95-96/148, September 10 – 13, 2018, Portoroz, Slovenia
- 2rd International congress on semiconductor materials and devices, 120/121, 28-30 Aug, 2018 Ardahan-Turkey
- VIII International Conference, Semipalatinsk Test Site: Legacy and Prospects for Scientific and Technical Potential Development, 161-162/174, 11–13 Sep 2018, Kurchatov, Republic of Kazakhstan
- International scientific conference of students and young scientists "Lomonosov-2018", Moscow, 2018, p. 34.14.1-3
- XXI Simposio Chileno de Física Antofagasta, SOCHIFI, Area H: Materia Condensada Fis. Estado Solido, Chile, 2018, p.SPH04.1-2
- 11th International Conference «Nuclear and radiation physics» 374/450, September 12-15, 2017, Almaty, Republic of Kazakhstan
- 26th International Conference Nuclear Energy for New Europe 302-55/197, September 4-7, 2017, Slovenia
- I International scientific conference of young researchers, Baku Engineering University, May 05-06, 2017, Baku, Azerbaijan
- 25th International Conference Nuclear Energy for New Europe, 602, 42-43, Sep 5-8, 2016, Slovenia

Publications: The main materials of the dissertation were published in 12 articles in high citation indexed journals and 7 abstracts at international conferences as well as, 11 articles and 5

abstracts at national journals and events. The main results of the dissertation are published in 35 scientific paper, including 23 articles and 12 abstracts.

Volume, structure and the main content of the dissertation:

The dissertation consists of an introduction, seven chapters, conclusions and references. 122 figures, 7 tables and overall 397210 symbols were used in the presented dissertation work.

THE SHORT CONTENT OF DISSERTATION

At the introduction the relevance of the topic of the dissertation, main purpose of the work, scientific novelty, practical significanceas well as, the main provisions to the defence are justified.

In the chapter I a summary of published scientific literature on the some physical properties, specific properties of various polytypes, technologies for obtaining nanoscale crsytalline materials and possibility application of silicon carbide compound in ionizing environments. Similar to other nanomaterials, has also been investigated that the physical properties of nanoscale silicon carbide slight different than macro-sized materials. Simultaneously, in general approach of this chapter general information are given about most common in different polytypes of silicon carbide and an overview of those which have amazing application capabilities. Also, the crystalline space structure of several poltypes including 3C-SiC polytype were comparatively analyzed. An order of atoms in different polytypes, possible inevatable defects in nanoscales and other crystalline properties have been interpreted according to known approaches in the literature. Moreover, possible modifications of the surface of particle in nanoscale and some processes occuring on the surface of nanoparticles have been interpreted in detail. In generl approach, application possibilities in ionizing environments and ionizing irradiation effects of silicon carbide were analyzed. Possible mechanical changes due to radiation in silicon carbide during the using at different temperatures in cosmic space, nuclear reactors as well as other ionizing environments have been elucidated based on

the literature. At the end of this chapter, the theme of the dissertation is substantiated according to the results of the discussions in the literature review

In the chapter II have been discussed neutron flux modification methods of nanocrystalline SiC particles, HRTEM, TEM, FESEM, SEM, SAED, EDP, EPR, study methods of electrical and dielectrical properties and devices. Explained the structure and irradiation techniques of the TRIGA Mark II type nuclear research reactor at the Institute of Jozef Stefan (IJS), used as a neutron source in experiments. The maximum power of the present TRIGA Mark II type reactor is 250 kW and the core located in the cylindrical aluminium tank with 2 m diameter and 6.25 m height. The core of the TRIGA Mark II type research reactor used as neutron source has a circular configuration. Thus, the core of the reactor, starting from the center, was composed of only six concentric rings. In generally, there are 91 possible positions inside the IJS TRIGA Mark II reactor, which can be used for various purposes, including positioning of neutron sources, control rods, irradiation channels and so on. The neutron flux density is $2 \times 10^{13} \text{ n} \cdot \text{cm}^{-2} \cdot \text{s}^{-1}$ on full power mode in the central channel (channel A1) where conducting the experiments. The photo and the schematic description of some parts of the reactor are given in figure (Figure 1).

An activity of nanomaterials increased approximately to 3GBq as a result of the influence of neutron flux and the reasons for this have also been investigated. k_0 -based Instrumental Neutron Activation Analysis (k_0 -INAA) method for studying the degree of purity of the 3C-SiC nanocrystals and the composition of trace elements are described in detail in this chapter.

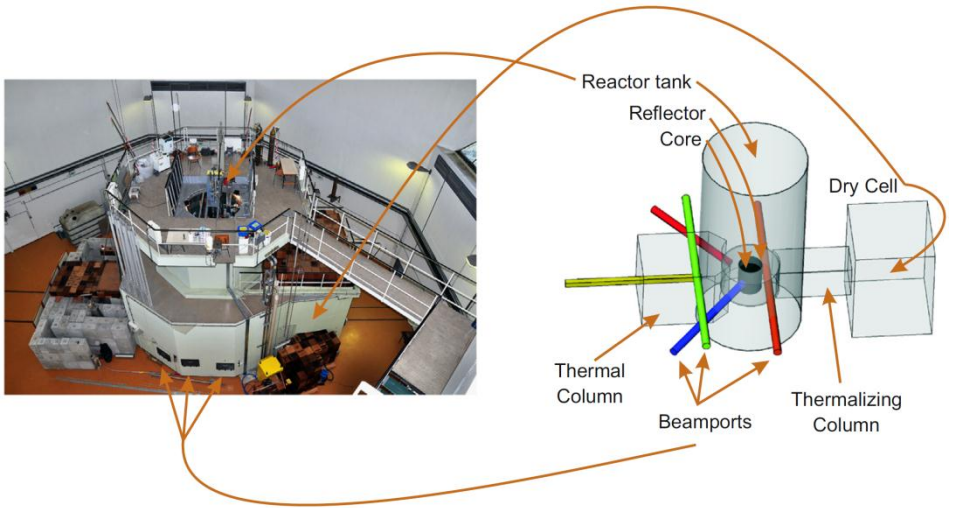


Figure 1. Photograph from the top of the reactor building and schematic description of the IJS TRIGA Mark II type research reactor.

HRTEM, TEM, FESEM, SAED, EDP and SEM methods used to study of structure, radiation defects, other ionizing irradiation effects on the 3C-SiC nanocrystals have been discussed in dissertation. Simultaneously, the DSC, DTA, TGA and TG methods used to study the thermal properties of nanomaterials are presented in this chapter. The method used to study of electrical and dielectrical properties of 3C-SiC nanocrystals also discussed in this chapter. Thats right, currently, there is no universal method for performing dielectric spectroscopy over a wide range of frequencies. However, there are certain methods for each interval, and each has its own advantages. The experiments were performed using the preferred method at selected intervals to achieve the goal in the dissertation work. In addition, the method used to study the current - voltage (C - V) characteristics of 3C-SiC nanocrystals is described in the chapter. A computer-coupled scheme of the system used to study both dielectric spectroscopy and current-voltage (C - V) characteristics is described. The devices used to study the current-voltage (C - V) characteristics were controlled by LabView and other similar

software and transferred to a computer for processing experimental results. The chapter also provides a schematic description of the EPR spectrometer used to study the defect and paramagnetic centers within the 3C-SiC nanocrystals. In the general approach, this chapter provides a schematic description of the devices and equipment used in all experiments.

All samples investigated in the dissertation were irradiated in the central channel by neutron flux. The central channel (Central Channel - CC) of the IJS TRIGA Mark II reactor is covered by aluminum tube. It should be note that the parameters of the existing neutron flux in the central channel at full power is $5.107 \times 10^{12} \text{ n}\cdot\text{cm}^{-2}\cdot\text{s}^{-1}$ (1 ± 0.0008 , $E_n < 625\text{eV}$) for thermal neutrons, $6.502 \times 10^{12} \text{ n}\cdot\text{cm}^{-2}\cdot\text{s}^{-1}$ (1 ± 0.0008 , $E_n \sim 625\text{eV} \div 0.1\text{MeV}$) for epithermal neutrons, $7.585 \times 10^{12} \text{ n}\cdot\text{cm}^{-2}\cdot\text{s}^{-1}$ (1 ± 0.0007 , $E_n > 0.1 \text{ MeV}$) for fast neutrons and finally the flux density in the central channel for all neutrons is $1.920 \times 10^{13} \text{ n}\cdot\text{cm}^{-2}\cdot\text{s}^{-1}$ (1 ± 0.0005). Other irradiation channels are also placed around the central channel with numbers F15, F19, F22, F24 and F26. Moreover, the triangular irradiation channel is installed in the situations of D8, E10 and E11. So that, the triangle irradiation channel are designed to irradiate relatively large size materials. In addition, there are several measuring slots inside the reactor with inner diameter from 8mm to 10mm to continuously study and control neutron flux density. So that the density and energy of the neutron flux are continuously measured and controlled. The core of the IJS TRIGA Mark II reactor is surrounded by the graphite reflector. There are slots in two parts for tangetial and radial beam tubes on the graphite reflector. Both beam tubes are placed in opposite position and serves two irradiation units, such as "thermal slot" and "thermal dry slot". Note that only thermal neutrons exist in both tubes and are considered to irradiate objects with larger physical dimensions.

It should be noted that the irradiation with neutron flux was carried out with using automatic transmission system for safety reasons. It is known that the samples have certain activity depending on the type when modified by neutron flux and it is dangerous to health working near it or instantly contact with the irradiated sample. Automatic irradiation robots are used to avoid instantly contact with

the sample irradiation. So that, sample is placed in the slot of the automatic transmission robot and remotely landed to the reactor channel using remote control. The samples are removed from the channel of the reactor with the same robots when the irradiation time has expired and the activity is always keeping under control. 3C-SiC nanocrystals were placed in the special plastic containers after irradiation. Only when the activity is below the permissible limit can it be approached and it can be transported anywhere from the hot area provided do not leave the hot area. Generally, it is important to make sure that the activity is below the permissible level of extraction from the hot area in order to conduct any other experiment on the sample. All these types of measurements and spectroscopic analyzes are carried out in hot areas and the samples can transport to other labs for further experiments after reduced activity.

The size and surface morphology of 3C-SiC nanocrystals were analyzed by HRTEM, TEM, FESEM and SEM methods. Simultaneously, the effect of the neutron flux on the structure of 3C-SiC nanocrystals were investigated by SAED, EDP and X-ray methods. TEM, SAED and EDP analyzes of the samples before and after neutron irradiation were conducted at “TEM, Jeol JEM-2010F” device at 200kV of effective voltage. The structure of the device and the research sequence are described in detail in this chapter. For the TEM analysis the samples were covered with copper-carbon then dried in the vacuum dryer and the measurements were conducted at high vacuum. Moreover, field emission SEM pictures of the samples were performed using “FE-SEM, Jeol JSM-7600” device on the 7 – 10 kV effective voltage and 8 mm working distance (WD) to study of agglomeration of initial and after neutron irradiated samples at relatively big sizes (about 200 nm). Unlike TEM studies, SEM analyzes were conducted directly in the vacuum without covering on the sample and to minimize environmental impact.

The thermal parameters of nanocrystalline 3C-SiC particles were investigated using “Perkin Elmer” STA 6000 device in the presented dissertation work. The working range on the “Perkin Elmer” STA 6000 device is 290K – 1273K, thermal processing rate are 5K/min, 10K/min, 15K/min and 20K/min, PolyScience analyzer

and “digital temperature controller” is cooling system. The kinetical parameters were determined using “Pyris Manager” software. The mass change and heat exchange occurred in the system can be measured using “Perkin Elmer” STA 6000 device. So that, the DSC, DTA, TGA and TG parameters of the sample can be easily study on this equipment. The “Perkin Elmer” STA 6000 device is supplied with a modern temperature sensor and mass recorder and this provides to perform perfect experiments. During the experiments, the argon gas was used to remove the combustion products from the system and prevent condensation. It is important to note that, at all experiments, argon gas was supplied to the system at a speed of 20 ml/min.

At this chapter, impedance spectroscopy method widely investigated for the study of neutron doping by impedance spectroscopy and for the interaction analysis of impedance spectra of 3C-SiC nanocrystals. The gold contacts were made by eruption method to the surface of the initial and after neutron irradiated samples in the special condition and performed quality control. Then the electrical and dielectrical properties of the samples were studied at “Novocontrol Alpha High Resolution Dielectric Analyzer” device for alternating current (AC~1V) in the ranges of 100 – 400 K temperature and 0.1Hz – 2.5MHz frequency. The temperature control accuracy was 10^{-2} K during the measurements and this accuracy was achieved by bridge method (Pt100 resistor). On the other hand, the current-voltage (V - A) characterisations were measured on the “Keithley 238 High Current Source Measurement Unit” equipment. In this case, all experiments were conducted in the range of -100V - +100V voltage with 5V steps at room temperature. Hysteresis measurement was performed (voltage from -100 V to 100 V and vice versa). Bottom side was placed onto the copper plate while the top side was contacted with a contact tip. Each sample was measured on three times where the position of the contact tip was changed.

In this chapter, EPR equipment, study method and sequence of performing experiments are explained in detail. Each of the obtained samples for EPR experiments was filled into high quality cylindrical quartz tubes about 50 μ l (1.5 mg) with 5 mm height and 2.5 mm

diameter. Note that the samples were irradiated by neutron flux at different times before filling into quartz tubes to reducing external effects. The EPR analyzes were performed on the “Bruker ELEXSYS E500 EPR spectrometer with high-Q resonator” equipment (Full sweep analysis, sweep = 500 G to 5500 G at center field of 3300 G = 0.33 T) for before and after neutron irradiation.

Chapter III is devoted to study of k_0 INAA, HRTEM, TEM, SAED, EDP, FESEM, SEM analyzes and structural properties of neutron irradiated nanocrystalline 3C-SiC particles. The radioisotopes of the trace elements formed in nano SiC under the neutron flux were studied as a function of time. Isotopes that dramatically increase the activity of samples as a result of neutron irradiation have been identified. The degree of purity of nano 3C-SiC particles synthesized by laser method have been determined by k_0 -based Instrumental Neutron Activation Analysis (k_0 -INAA) method. As results of activation analyze after irradiation, the composition of trace elements in nano SiC was determined by the radionuclides of the corresponding elements. The percentage of mixed radioisotopes has been determined by k_0 -INAA method.

Long lifetime radionuclides were analyzed during the twenty days (about 500 hours). In general, here 8 types of radionuclides were observed which the half-life changes from 12.7 hours to 8.6E8 h. Analysis shows that radionuclides with relatively long lifetime can be classified into two distinct groups based on their initial activity. The first group includes radionuclides with an activity of about 0.35kBq. The half-life of radionuclides in this group are 1023 hours (^{181}Hf), 1077 hours (^{59}Fe), 7508 hours (^{54}Mn), $5.8 \cdot 10^8$ hours (^{93}Zr), $6.7 \cdot 10^8$ hours (^{59}Ni) and $8.6 \cdot 10^8$ hours (^{41}Ca). The activity of all radionuclides was almost less than 0.35kBq after about twenty days. The second group includes two radionuclides with long lifetime. The initial activities of these radionuclides is about 163 MBq. The half-life of observed radionuclides in this group are ^{64}Cu 12.7 hours and ^{24}Na 15 hours, respectively. The activity of both radionuclides were reduced to zero after twenty days due to the relatively short half-life of these radionuclides.

The initial activity of other radionuclides with short lifetime is

approximately 54MBq. Here two types of ^{52}V and ^{27}Mg radionuclides were observed which the half-life was 0.062 hours for ^{52}V and 0.16 hours for ^{27}Mg , respectively. Experimental analyzes show the activity of both radionuclides decreases to zero that after 5 hours. The initial activity was approximately 3GBq in the other group short lifetime radionuclides. In the initial approach assumed that the main source of high activity is the ^{38}Cl isotope. The half-life of observed high activity ^{38}Cl isotope is 0.62 hours and the activity of this isotope was reduced from 3GBq to about 11.5kBq after 5 hours. The initial activity of ^{28}Al isotope in this group is 1.4GBq with 0.037 hours half-life (the activity of ^{28}Al isotope was reduced to zero after 5 hours). It was found that the ^{38}Cl isotope which is several times more active than others is the main part of the mixture.

Generally, percentages of newly formed total radioisotopes as a result of neutron irradiation, mainly the initial isotopes and the number of neutrons absorbed by these isotopes, are detailed in the work. Simultaneously, it should be considered that the indicated values of the concentrations of Al and Mg isotopes may be slightly less than the obtained results from the low probability of the $^{28}\text{Si} (n, p) \rightarrow ^{28}\text{Al}$ and $^{30}\text{Si} (n, \alpha) \rightarrow ^{27}\text{Mg}$ reactions. However, in order for these reactions to occur, the minimum energy of neutrons participate in the process must have at least 4 MeV. The average energy of neutrons in the reactor performing experiments varies about around 1MeV, but the existence of neutrons with energy greater than 4 MeV is inevitable. Thus, the concentration of Al and Mg may be less than 0.015% and 0.0083%, due to possible nuclear reactions.

The nanomaterial was investigated by SEM and TEM devices before and after neutron irradiation. Agglomeration of nanoparticles were comparatively studied before and after irradiation. Dimensions of the nanoparticles used in the experiments were investigated by SEM analyzes. Amorphization the surface of the nanoparticles was analyzed at TEM device. The defect and other effects of neutron irradiation on nanocrystalline 3C-SiC particles also studied by TEM device. The influence of the neutron irradiation on the crystal structure was studied using SAED and EDP analyzes. From TEM analyzes, it was revealed that the neutron irradiated sample exposed

more agglomeration than the initial sample. Comparative TEM images before and after irradiation at greater magnification are given in Figure 2. As can be seen from the figure, the amorphous layer about with 3 nm thickness is formed on the surface of nanoparticles during the neutron irradiation. It is assumed that this amorphous layer (3nm thickness) either can be displacements of several lattice atoms on the surface under the influence of the neutrons or oxidizing some atoms on the surface.

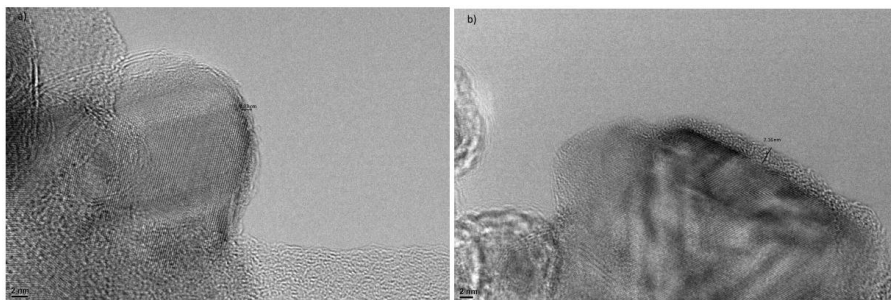


Figure 2. TEM images of nanocrystalline SiC particles before (a) and after (b) neutron irradiation (about 3 nm amorphization on the surface after irradiation)

Moreover, comparative analyzes shown that the number of the “spot” increases after irradiation (compared to non-irradiated samples) (Figure 3). The atoms in the crystal lattice were observed by high-sensitivity magnification at TEM device (HRTEM – with 2 nm index) and confirmed the nanocrystalline nature of the material (Figure 2 and Figure 3 a, c). The increases of the possible formed “spots” in the crystal as a result of the influence of neutron flux are more clearly noticeable in the magnifications that can be observed of the lattice atoms (Figure 3c). The defects or clusters formed on the nanomaterial irradiated by neutron flux are explained by “spots” observed at HRTEM images.

Both diffraction views (Figure 4) were analyzed by rotation average (RA) with which increase the sensitivity rate of the intensity. Both diffraction views were comparatively analyzed before and after

neutron irradiation (Figure 4). EDP ring patterns were analyzed in Gatan's Digital Micrograph software package.

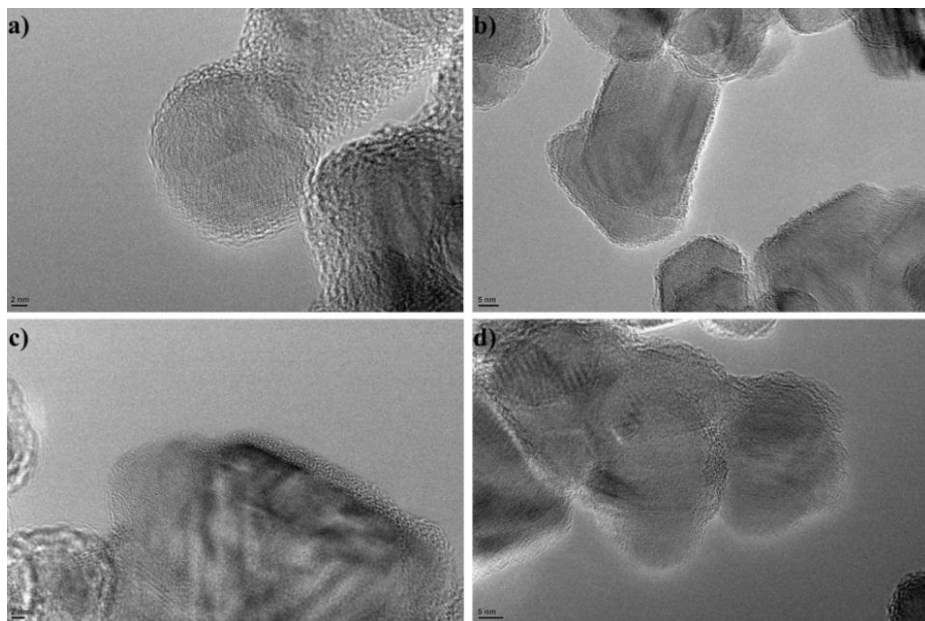


Figure 3. TEM images of nanocrystalline 3C-SiC particles before (a and b) and after (c and d) neutron irradiation.

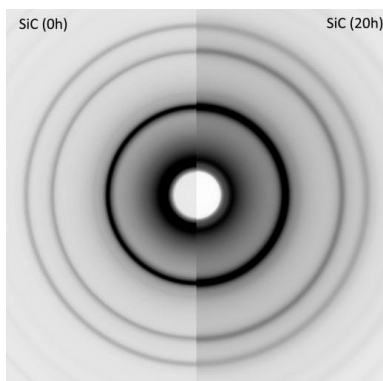


Figure 4. Comparison of rotation average (RA) of EDPs between 3C-SiC (0 h) and 3C-SiC (20 h).

The (*h k l*) parameters of nanocrystalline SiC particles were determined by x-ray analyzes. The presence of other modifications of polytypes of the silicon carbide in the sample was investigated. 2 θ angles are defined according to the lattice parameters. The values of the lattice parameters and lattice angles were determined for nanocrystalline 3C-SiC particles.

In chapter IV, the capturing, scattering, and formation of defect states of neutron flux in nanocrystalline 3C-SiC particles are reviewed by computer modelling and optimal neutron energies are evaluated according to the purpose of the dissertation. Modelling of a general characterization of the interaction between neutron flux and nanocrystalline 3C-SiC particles are examined. The absorption of neutrons in nanocrystalline 3C-SiC particles at various energies studied using computer modeling. Absorption of neutrons in nanomaterial has been studied separately for the silicon and carbon atoms in the 3C-SiC particles. Since the effective cross-section of absorption is different in various isotopes of silicon and carbon atoms the modeling for each stable isotope were performed separately. Simultaneously, the effective cross-section spectra of neutron capture for silicon and carbon atoms were mutually investigated. The resonance state in the stable isotopes of silicon (^{28}Si , ^{29}Si and ^{30}Si) occurs at around 0.1MeV of energy (Figure 5b and c). As seen from the absorption of neutron flux spectra, the resonance states observed in the absorption spectra shift towards energy reduction with the increase in the mass number of stable isotopes of the silicon. In other words, if the minimum energy of resonance state observed in the absorption spectrum of ^{28}Si is about $5 \cdot 10^{-2}$ MeV, this value of energy for ^{29}Si and ^{30}Si isotopes are 10^{-2} MeV and 10^{-3} MeV, respectively. This indicates that occurring of resonance states at lower energies is possible with increasing the mass number of the silicon isotope. Note that, unlike other stable silicon isotopes, the absorption spectrum resonance in the ^{30}Si isotope has a great practical importance. Thus, the ^{30}Si isotope is responsible for the neutron transmutation. The transformation to ^{31}Si isotope by neutron capture in the ^{30}Si isotope and transformation it into the ^{31}P isotope by β -decay causes fundamental changes in the

physical properties of nanocrystalline 3C-SiC particles. Thus, the ^{31}P isotope is n-type dopant in nanocrystalline 3C-SiC particles and its concentration has a great practical importance in the electronic systems. On the other hand, the nanocrystalline 3C-SiC particles are very important for the study of neutron capture in carbon atoms as a result of their interaction with neutrons. During the interaction between neutron flux and ^{12}C atoms, the resonance state is not observed up to 20 MeV of the energy of neutron. However, the resonance state is observed in ^{13}C isotope around 10^{-1}MeV of energy. This suggests that the nanocrystalline 3C-SiC particles can increase the concentration of ^{14}C isotopes due to the capture of neutrons with 0.1MeV energy. The ^{14}C isotope is β -active which transforms to ^{14}N isotope at certain time. The less concentration of ^{13}C and low probability for forming ^{14}C isotopes than other processes are the main reasons for disavowal these processes in the experiments. The comparative analysis has shown that the effective cross-section of neutron capture for Si isotopes is approximately 10^3 times greater than C atoms.

Simultaneously, (n, p) and (n, α) transmutations formed in nanocrystalline 3C-SiC particles by neutrons with different energies were investigated. Possible (n, p) and (n, α) transmutations under the influence of neutron flux were studied separately for silicon and carbon atoms in the 3C-SiC nanoparticles. The effective cross-section of the probability of (n, p) and (n, α) transmutations in different type isotopes of silicon and carbon atoms are different and therefore, each stable isotope was examined separately. The spectra of the effective cross-section of (n, p) and (n, α) transmutations for silicon and carbon atoms were mutually studied. Si isotopes are turned to corresponding Al isotopes during the (n, p) transmutations. $^{28}\text{Si}(\text{n}, \text{p})^{28}\text{Al}$ transmutation for ^{28}Si isotope becomes more intensive at the certain energy range. However, there is a minimum border value of energy that (n, p) transmutation does not occur at smaller energies. This value of energy is characterized with Q-factor. The value of the Q-factor varies widely depending on the type of nuclear transformation. On the other hand, the Q-factor maybe both positive ($Q > 0$, while the transformation is exothermic) and negative ($Q < 0$,

when the transformation is endothermic), depending on the type of nuclear interaction. In particular, the Q-factor is zero if the nuclear interaction is elastic. The process is endothermic ($Q < 0$) when using the energy of neutron for (n, p) and (n, α) transmutations. In other words the energy is absorbed from outside when (n, p) and (n, α) transmutations (the energy of neutrons in given case). With this approach, we can say with the slight error that required minimum energy of neutrons equal to the module of the value of Q-factor for the occurrence of (n, p) and (n, α) transmutations. Minimum energy of neutrons were 3.86 MeV for occurrence of (n, p) transmutations on ^{28}Si isotopes and was intensive up to 20 MeV of neutrons energy. The resonance condition exists about 8 MeV – 15 MeV of energy range. The minimum energy of neutrons to the occurrence of $^{29}\text{Si}(n,p)^{29}\text{Al}$ transmutations on ^{29}Si isotopes was evaluated around 2.9 MeV. The resonance condition for ^{29}Si exists around 10MeV of energy. $^{30}\text{Si}(n,p)^{30}\text{Al}$ transmutations on ^{30}Si isotopes can occur by 7.75 MeV energy of neutrons. The resonance condition for $^{30}\text{Si}(n,p)^{30}\text{Al}$ transmutations exists about 8MeV-20MeV energy range. Moreover, Si isotopes can be transmuted to corresponding Mg isotopes by (n, α) transmutations. The minimum energy of neutrons to the occurrence of Mg transmutations on ^{29}Si isotopes was evaluated around 2.65 MeV and the resonance condition around 10MeV of energy. Similar calculations were carried out in the condition of neutron flux scattering from nanocrystalline 3C-SiC particles. Simultaneously, elastic, nonelastic and inelastic scatterings and general effective cross-section were considered for each stable isotope.

Unlike other stable isotopes of the silicon, the numerical value of the effective cross-section of elastic and inelastic scattering on ^{30}Si isotopes is greater (Figure 6a and c). Nevertheless, effective cross-section of non-elastic scatterings is low probability process and corresponds to the other stable isotopes (Figure 6b). The value of general effective cross-section mainly corresponds to the numerical values of the effective cross-section of elastic and inelastic scatterings. This means that elastic and inelastic scatterings are also predominant on the ^{30}Si isotopes. This is the result of the inelastic

scattering that nanocrystalline 3C-SiC particles are doped with ^{31}P isotopes and improve physical properties.

It should be noted that the effective cross-section of scatterings for low energy neutrons from ^{12}C isotopes in the nanocrystalline 3C-SiC particles are low probability processes. For this reason, the effective cross-section for the ^{12}C isotope has been considered at the bigger energy neutrons. So that, the elastic, non-elastic, inelastic and total effective cross-section for ^{12}C isotope have different character up to 20 MeV of neutron energy. The numerical value of effective cross-section of elastic scattering is also high in the ^{12}C isotope as in other isotopes and this case is more probable process. On the other hand, the numerical values of the effective cross-section of non-elastic and inelastic scatterings are very small and are low probable processes. Numerical values of the total effective cross-section is more relevant with the numerical value of elastic scattering. However, there is a difference between the effective cross-section of elastic scattering and total effective cross-section and this is relatively negligible to say that the process consists mainly of elastic scattering. Nevertheless, we can say that the main part of the process is due to elastic scattering. Also, the effective cross-section for ^{13}C isotope was modeled despite low mass fraction. It was defined from effective cross-section of neutron flux for ^{13}C isotope that the elastic scattering is preferable. The numerical values of the effective cross-sections of non-elastic and inelastic scatterings are very small and low probable processes. Total effective cross-section is almost the same as the effective cross-section of elastic scattering. This confirms that the main part of the process occurs with elastic scattering.

On the other hand, the defects with different nature formed in nanocrystalline 3C-SiC particles under the influence of the neutron flux were studied by computer modelling. Space structure and possible defect conditions by neutrons in nanocrystalline 3C-SiC particles were investigated using special programs. Simultaneously, most probable energies of neutrons to forming defects were calculated. The probability of formed Si and C voids under the influence of neutron flux at lattice atoms have been evaluated. It was

found that most probably point defects forms in nanocrystalline 3C-SiC particles around the 5 MeV of the energy of the neutrons.

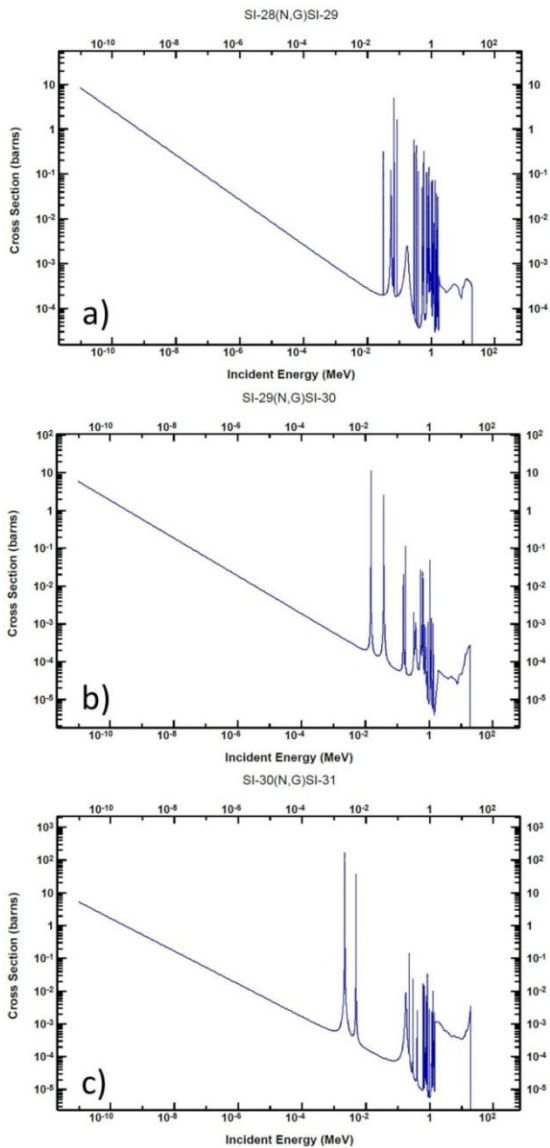


Figure 5. Effective cross-section spectra of the neutron capture in different stable isotopes of silicon.

Cubic modification SiC nanoparticles consist of Si and C atoms and high energy scattering (high energy recoils, primary knock-on atoms – PKA) can be observed at some atoms under the influence of neutron flux on the lattice atoms. The point defects and clusters form during energy exchange between PKA atoms and other neighboring atoms and these also form the basis of fundamental defects. Let's consider the possible PKA formation in nanocrystalline 3C-SiC particles during neutron irradiation. It's known that after neutron irradiation, PKA refers to the first atom in which directly interact with neutrons. In this case, PKA may release one or more atoms in the lattice depending on the storage energy in the crystal lattice of the falling neutrons and the target atom. In a sense, the forming of PKA states is equivalent to the forming of Frenkel pairs. So that, the atoms leaving the lattice in one process, the first is called PKA, and the other can create Frenkel pairs, including the initial atom. The energy of the neutrons must be greater than the full multiplier of the atomic energy of the lattice atoms for a couple of Frankel pairs formed at the PKA case. In other words, if the boundary energy of the lattice atoms is E , the minimum energy of neutron for the formation of Frankel pairs from PKA should be $2E$, $3E$ and so on.

The formation of the possible voids by Si and C atoms in the nanocrystalline 3C-SiC particles under the influence of neutron flux is possible only when the energy of the neutrons is sufficient to extract of the isotope from the crystal lattice without any nuclear transmutation. The probability of emergence of corresponding voids decreases to zero if any (n,p) , (n,α) or other nuclear transmutations occurs in the process. In the general approach, it is usually necessary for any of the (n, γ) or (n, n') nuclear reactions to form defects during neutron irradiation. The probability of these types of nuclear reactions is characterized by effective cross-section directly characteristic for each nucleus. So that, the (n,γ) and (n,n') nuclear reactions were separately analyzed for each stable isotopes due to the different effective cross-section in the different stable isotopes (natural composition is 92.23% ^{28}Si , 4.67% ^{29}Si and 3.1% ^{30}Si for Si and 98.93% ^{12}C and 1.07% ^{13}C for C) of Si and C atoms that form

the nanocrystalline 3C-SiC particles.

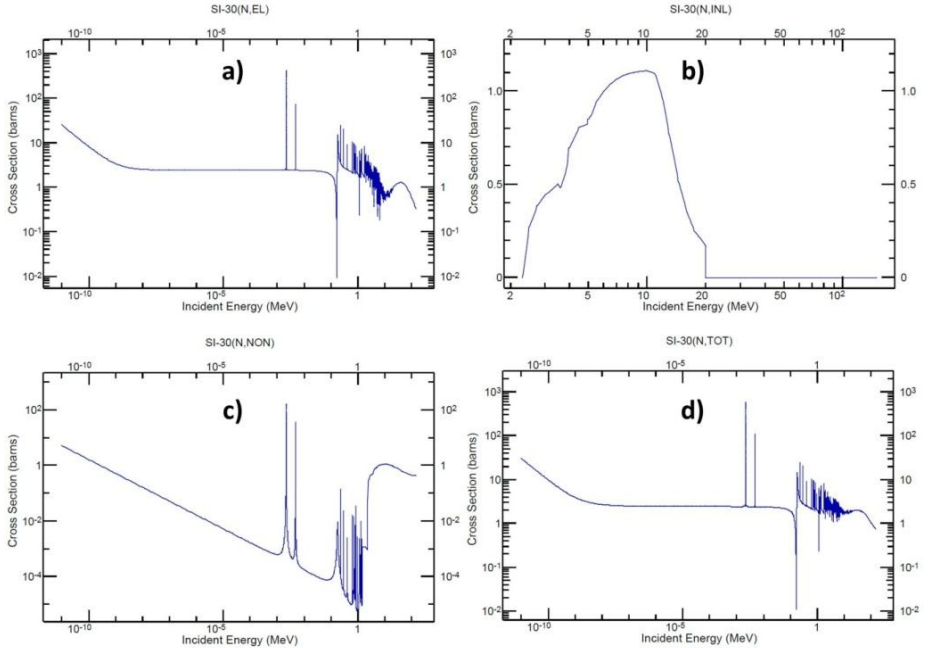


Figure 6. Elastic (a), non-elastic (b), inelastic scattering and general (d) effective cross-section spectra of neutron flux for ^{30}Si isotope.

It is known that the theory of the formation of cascade states during the neutron irradiation is explained as the neutrons with the certain energy excite isotope when interacting with any atom and excited isotope transfers energy to the surrounding atom with exciting neighboring atoms. Note that the formation of the cascade states in 3C-SiC nanocrystal under the influence of the neutron flux is not only with (n, γ) and (n, n') also formed by the interaction of neutrons with Si and C atoms. Also, the emergence of point or other types of defects is not only with (n, γ) and (n, n') nuclear reaction, in general, formed by the interaction of the neutrons with any types atoms.

In chapter V, the influence of neutron flux on the electrical properties of nanocrystalline 3C-SiC particles and formed new

effects resulting from irradiation are described in details. In first, cubic modification silicon carbide (3C-SiC) nanomaterial with 18 nm particle size was irradiated by neutron flux at different duration. Frequency dependences of electrical conductivity and effect of the neutron flux comparatively studied in the work. In the initial case, frequency dependences of electrical conductivity of 3C-SiC nanoparticles irradiated at different times by neutron were considered in the range of 100K – 400K temperature. Measurements were conducted at each temperatures in the range of 0.1Hz to 2.5MHz. As a result of neutron irradiation, there was observed conductivity (radiation-induced conductivity – RIC) in the 3C-SiC nanoparticle due to the neutron irradiation and this conductivity has been investigated as a function of frequency. The type of conductivity from the interdependence of real and imaginary parts of electrical conductivity is defined. Simultaneously, the influence of the temperature and neutrons on the electrical conductivity of nano 3C-SiC irradiated with neutron flux were studied different frequency range. It was determined that there are formed additional electro active defects under the direct influence of the neutrons or under the influence of the beams emitted by any other activated isotopes. So that, the change of neutron flux at the range of $6,7 \times 10^{17} \div 2,7 \times 10^{18}$ n/cm²s increases the electrical conductivity of nano 3C-SiC. It has been shown that the main reason for the increase in the numerical value of electrical conductivity is new ³¹P isotopes formed in the nanomaterial as a result of the neutron transmutations. Activation energies of the samples were calculated before and after neutron irradiation for two different constant values of frequency using Arrhenius approach. The mechanism to explain obtained results has been proposed.

Due to the 20 hours neutron irradiation, additional conductivity (radiation-induced conductivity RIC) formed in the nanocrystalline 3C-SiC, which is were calculated in the frequency range of 0.1Hz – 2.5MHz at different temperatures (Figure 7). RIC conductivity was calculated for 20 hours of neutron irradiated sample using $\sigma_{0h} - \sigma_{20h}$ (difference) and σ_{20h}/σ_{0h} (ratio) approaches. Here, σ_{0h} and σ_{20h} are experimental values of electrical conductivity before and after 20

hours neutron irradiated of nano 3C-SiC, respectively.

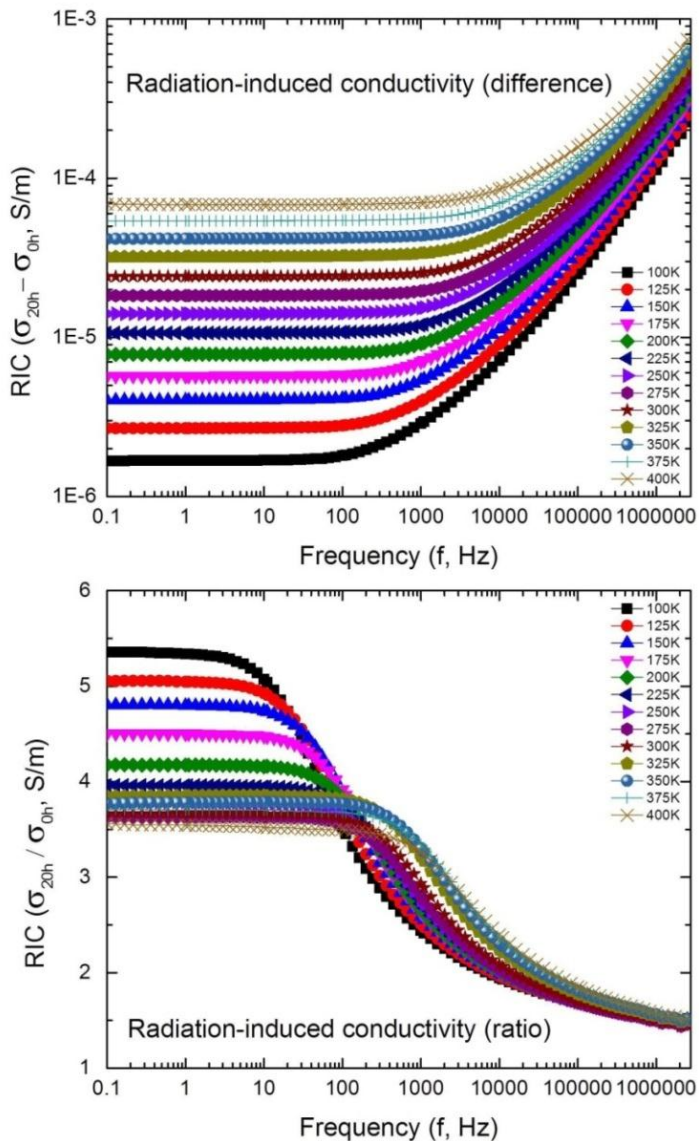


Figure 7. Frequency dependencies of RIC (difference, a) and RIC (proportional, b) conductivities of 3C-SiC nanomaterial at the different temperatures

From the frequency dependence of RIC (difference) conductivity have been determined that the radiation effects do not depend on the frequency in the range of $f < 1\text{kHz}$ (Figure 7a). However, RIC (difference) conductivity is linearly increased depending on the frequency in the range of $f > 1\text{kHz}$. On the other hand, RIC (difference) conductivity increase depending on the temperature. So that, the RIC (difference) conductivity is $2 \times 10^{-6}\text{ S/m}$ at 100 K of temperature, but this value is increased up to $8 \times 10^{-5}\text{ S/m}$ at 400 K of temperature. Note that, this difference has a smaller value in the high-frequency ranges.

In the general approach, it was determined from experiments that, the maximum value of RIC conductivity formed in the samples as a result of the influence of neutron flux about $7.5 \times 10^{-4}\text{ S/m}$. RIC (difference) conductivity get the highest value at the maximum values of temperature and frequency. From this, we can conclude that neutron flux forms more charge carriers at higher frequencies and temperatures in nanomaterials. Relative conductivity is less observed at higher frequencies (Figure 7b). Relative conductivity does not depends on frequency at low frequencies (according to the RIC difference). It is known from frequency dependencies of relative conductivity that RIC (proportional) has a minimum value at the maximum value of frequency (1.5 times increasing). The maximum increasing at relative conductivity is observed low frequencies range at 100 K of temperature (5.5 times increasing).

As a result of measurements at all temperatures, it was found that the electrical conductivity of the 3C-SiC nanomaterials almost not depends on the frequency at small frequencies. However, additional carriers within the nanomaterials as a result of neutron irradiation in the low-frequency range causes to obviously observed of the neutron effects. Active participation of existing charge carriers or electrons at local states in the conductivity is possible as a result of the neutron irradiation. This cause to increase in the numerical value of electrical conductivity of the 3C-SiC. Furthermore, the effect of the external electric field in the high-frequency ranges exceed the neutron effects. As a result, at high frequencies, the neutron effects are observed small, but the frequency effects of the electric field are

observed more. Moreover, there was a shift of the stable region in the direction of the increase of conductivity with increasing temperature. The main reason for this the numerical value of conductivity increase with the influence of temperature. Thus, the temperature effects exceed the corresponding frequency effects at relatively high temperatures.

The electrical activation energy of nano 3C-SiC were calculated basis on the obtained results using Arrhenius approach before and after neutron irradiation. The slope in the $1000/T$ dependence of natural logarithm of electrical conductivity represents the activation energy. The calculations were carried out for two frequencies (0.1 Hz and 2.5 MHz). There was observed an increase in activation energy with increasing the temperature ($T_{p1} < T_{p2}$). The numerical values of the activation energy obtained in accordance with the calculations are detailed in the work. It was revealed that the numerical value of activation energy increase with increasing the neutron irradiation time in all cases. This can be explained by the increased concentration of additional charge carriers or trace elements formed within the sample as a result of neutron irradiation. There was also a decrease in activation energy with increasing frequency. This is due to the active participation of charge carriers in the deeper levels at relatiely higher frequencies.

Moreover, in this chapter, the impedance spectra of the nanocrystalline 3C-SiC particles have been comparatively analyzed before and after neutron irradiation. Observed resonance conditions and shifts on the impedance spectra of nanocrystalline 3C-SiC particles after neutron irradiation have been explained by different approaches. The relaxation times have been calculated from the interdependence of real and imaginary parts of the impedance of nanocrystalline 3C-SiC particles. Calculated relaxation times have been analyzed as the function of neutron irradiation time. The influence of ^{31}P isotopes formed as a result of the neutron transmutations in the nanocrystalline 3C-SiC particles on impedance spectra have been analyzed. In addition, the influence of the amorphization or agglomeration of nanocrystalline 3C-SiC particles on polarization rate and relaxation time have been analyzed using

HRTEM, TEM and SEM methods. Simultaneously, in this chapter, the impedance spectra of the nano silicon carbide (3C-SiC) were studied as the function the temperature at the initial case and continuously irradiated by neutron flux at different times. Impedance spectra of the sample were investigated in the frequency range of 0.1Hz – 2.5MHz and the temperature range of 100K – 400K. Temperature dependencies of the impedance spectra of samples were comparatively investigated before and after neutron irradiation. The nature of the conductivity and the temperature of metal-semiconductor transition were determined using complex impedance spectroscopy. There was observed increasing in polarization by increasing the time of the influence of neutron flux. Mechanisms of all effects observed in experiments are given.

Impedance spectra were considered in general case before and after irradiation at different values of temperatures (Figure 8). As can be seen from the image, there are peak states in the real and imaginary parts of the impedance of nanocrystalline 3C-SiC particles before and after neutron irradiation. As seen from the frequency dependence of the real part of impedance that the numerical value of impedance increase by increasing temperature and frequency (Figure 8a, c). This cause to change of other physical properties under the influence of temperature and frequency. There is also jumping transition at certain frequency, which can be regarded as the current relaxor condition at that frequency. Similar jumping case are observed at imaginary parts of the impedance of nanocrystalline 3C-SiC particles (Figure 8b, d). On the other hand, the shifts were observed in the direction on the increase of frequency on impedance spectra after neutron irradiation (Figure 8c, d). Simultaneously, the numerical value impedance of nanocrystalline 3C-SiC particles increases up to 5.5 times as a result of the neutron irradiation. The reason for observed decreasing and shifts at the impedance spectra as a result of the neutron irradiation are explained by trace elements or additional charge carriers formed in nanocrystalline 3C-SiC particles as a result of the neutron irradiation.

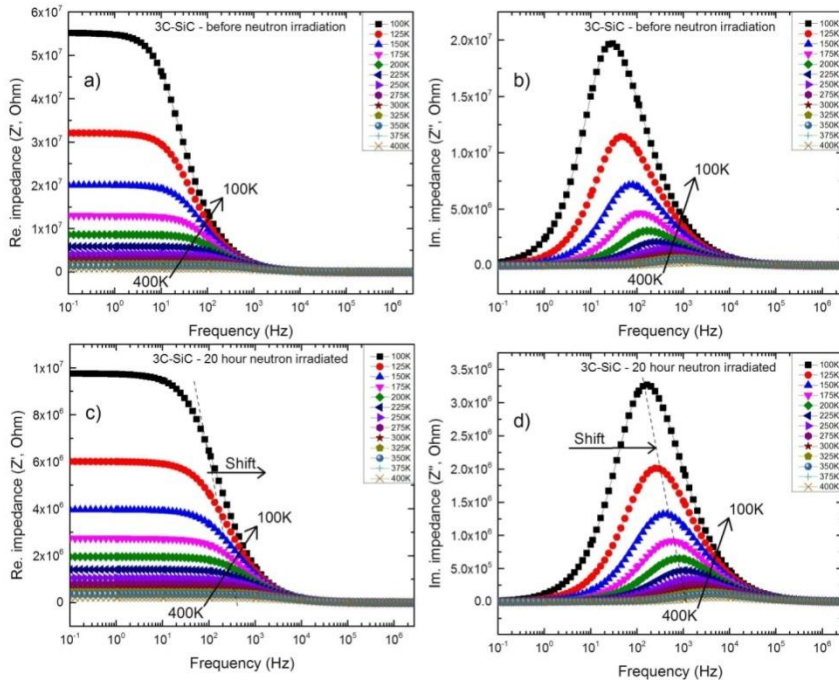


Figure 8. Impedance spectra of nanocrystalline 3C-SiC particles before and after neutron irradiation.

Neutron irradiation effects are clearly seen from the interdependence of real and imaginary parts of impedance at different constant temperatures before and after neutron irradiation (Figure 9). There are observed decreasing of the impedance of nanocrystalline 3C-SiC particles at all temperatures by the influence of the neutron flux. This, directly impact to physical properties of nanocrystalline 3C-SiC particles. The Cole-Cole approach is one of the compatible ways to explain these types of curves obtained from experimental results. The results of the experiments can be summarized in general by the following Cole - Cole equation:

$$Z^* = R_\infty + \frac{R_0 - R_\infty}{1 + (i\omega\tau)^{1-h}}$$

where R_0 - R_∞ is nominal, called space constant, R_0 and R_∞ are resistivities at low and high frequencies, respectively, h – parameter characterized the distribution of relaxation time. During the monodispersive relaxation, $h = 0$ and $0 < h < 1$ shows the distribution of the relaxation time in the system. The h parameter can only be determined from the central position with the above parts of arc in the Cole - Cole diagram. As can be seen from Figure 9 the polydispersity of the relaxation spectrum increases by increasing neutron irradiation time. Obtained results are acceptable and this shows that the process can be well explained by single relaxation time. The relaxation times of nanocrystalline 3C-SiC particles were calculated at different constant temperatures according to Cole-Cole diagrams.

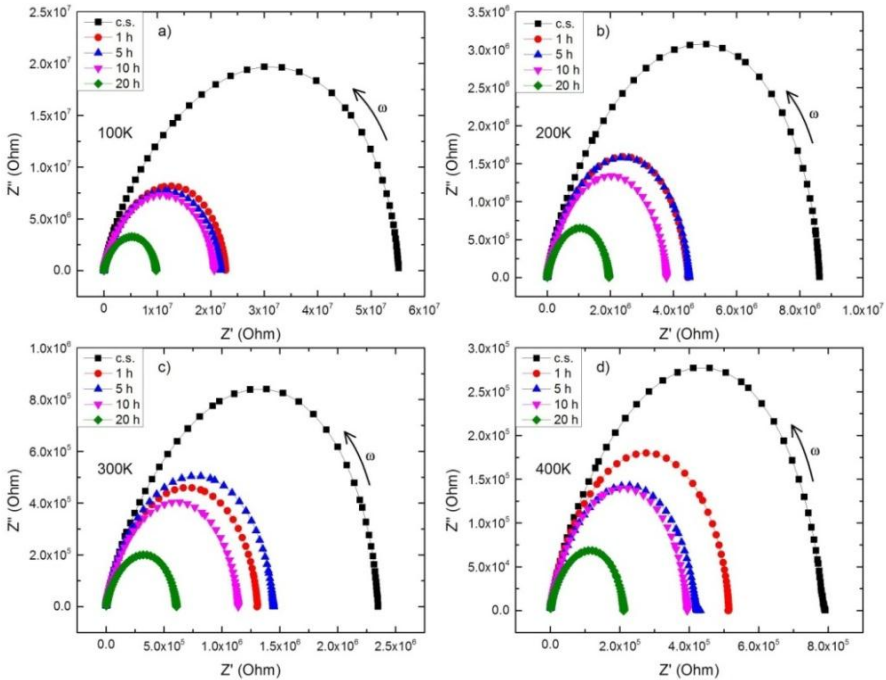


Figure 9. Comparative dependencies of real and imaginary parts of the impedance of nanocrystalline 3C-SiC particles at different constant temperatures (100K, 200K, 300K and 400K) before and after neutron irradiation

The temperature dependencies of the impedance have a different character in average frequency intervals. At the 1kHz of frequency, almost linearity is observed in the $f(Z)=f(T)$ dependencies. Simultaneously, the numerical value of Z' increase by increasing the influence of the neutron irradiation time and temperature. The numerical value real part of the impedance increase by increasing the temperature up to 250 K at relatively high frequencies (0.1 MHz). Characterical decreasing are observed on the $f(Z)=f(T)$ dependencies between 250K – 400K temperature interval. The analogical case is also observed at relatively high frequencies. An increasing of the frequency cause to changes in the impedance spectra because the bandgap of 3C-SiC nanocrystals is 2.2 eV. It is possible that the electron conductivity in the 3C-SiC nanocrystals prevails (metal transition) at relatively high frequency. For this reason, the numerical value of the impedance at 0.1MHz, 1MHz and 2.5MHz of frequencies have characteristic of metallic materials up to 250K, 325K and 370K of temperature, respectively. So that, the numerical value of the real part of impedance increase by increasing temperature at 0.1MHz, 1MHz and 2.5MHz frequencies. Moreover, the impedance decreases by increasing temperature after the certain temperature corresponding to the semiconductors. This can be explained that. This can be explained by the fact that the charge carriers are metallic nature up to the certain value of temperature.

There are observed characteristic properties to semiconductors after 250K, 325K and 370K of temperature. The values of 250K, 325K and 370K of the temperatures have been evaluated as metal-semiconductor transition (T_{MS}) temperature for 3C-SiC nanocrystals. Thus, the metal-semiconductor transition is observed on 3C-SiC nanocrystals according to the 0.1MHz, 1MHz and 2.5MHz of frequencies at $T_{MS} = 250K, 325K$ and 370K temperatures, respectively. Simultaneously, the numerical value of T_{MS} are shifted to the direction of low temperatures with increasing the influence of neutron irradiation time. This can be explained by neutron transmutation, dangling bonds and formed defects or additional charge carriers.

On the other hand, V – A characteristic in the tension range of -100 - +100V with 5V steps of 3C-SiC nanocrystals were considered in this chapter. The angular shift was observed on V – A characteristic of nanomaterial with increasing neutron irradiation time. At the same time, it was determined that the resistivity of the 3C-SiC nanocrystals decreased about from 4 MΩ to 1 MΩ after neutron irradiation. Moreover, it was determined from Fowler–Nordheim dependencies that the processes occurred in the 3C-SiC nanocrystals are directly based on tunnel phenomenon and field emission does not observe. Fowler–Nordheim dependencies have shown that the thermal activity is dominant in the 3C-SiC nanocrystals before and after neutron irradiation.

Studies have shown that the V – A characteristic of the sample before neutron irradiation is sloping at a small angle relative to the linear and voltage axis, indicating that the initial sample has relatively high resistance. Simultaneously, the symmetry of the line relatively to zero point of the voltage and current axes indicates high purity of the samples. However, the slope changing are observed on the V – A characteristic of nanomaterial with increasing impact duration of the neutron flux. So that, the angle between curves observed on the V – A characteristic and voltage axis before and after neutron irradiation of 3C-SiC nanocrystals is sharply increased after neutron irradiation. On the other hand, it is known that the cotangent of the angle is directly characterized the resistance of the sample: $\cot\alpha = R$. An increasing of angle between curves and voltage axis after neutron irradiation cause to decrease of the sample resistance. Thus, the electrical conductivity of the samples increases under the influence of the neutron flux which has been confirmed in the experiments. Similar to previous experiments, this increase can be explained by neutron transmutations, dangling bonds, defects or additional charge carriers. The shifts in the dependencies of current-resistance and voltage-resistance were observed with the influence of the neutron flux.

In chapter VI, the influence of the neutron irradiation on the dielectrical and paramagnetic properties of nanocrystalline 3C-SiC particles have been investigated in details. Dielectrical properties of

3C-SiC nanoparticles were considered in the range of 0.1Hz-2.5Hz frequency and 100-400K of temperature. The real and imaginary parts of the permittivity were comparatively analyzed for initial and neutron irradiated nanomaterial. As a result of the analyzes, it was determined that the permittivity of nano SiC increase under the influence of the neutron flux. It was defined that additional trace elements are formed as a result of the effect of neutron flux. An increase of new trace elements formed in the 3C-SiC nanomaterial is directly influence on the dielectrical plarization. Moreover, the polarization of 3C-SiC nanoparticles on the intermediate surface (nanoparticles interfaces) cause to forms of the dispersion states. It was defined that ionic polarization in the nanocrystalline 3C-SiC particles is predominant. The mechanism of the observed peaks and other effects are given based on the obtained experimental results. Moreover, the temperature dependencies of the real and imaginary parts of permittivity of cubic modification nano silicon carbide (3C-SiC) which in the initial state and continuously irradiated by neutron flux in different times are detailed examined. Temperature dependencies of the real and imaginary parts of permittivity of the samples were studied before and after neutron irradiation. Neutron irradiation effects were investigated comparatively with non-irradiated samples. There was observed increase of the polarization with increasing of the neutron flux duration. Two dispersion regimes are observed at low and high temperatures. The dispersion states observed at low frequencies can be explained with surface carriers basis on the polarization phenomena or polarization in the nanoparticles interfaces. High frequencies can be expalined by relaxation process associated with the charge carriers mobility. The real and imaginary parts of dielectric permittivity were considered on the one coordinate system. The dielectric loss factor (ϵ'') is dominated at low frequency ranges. The real and imaginary parts of dielectric permittivity are dominated at relatively high frequencies. In general approach, this type of dependence is typical for materials which have ionic charge carriers. Hopping conductivity and collecting of charge carriers in traps are acceptable in these types of dependencies. In all cases, the real and imaginary parts of dielectrical

permittivity curves are intersect in the range of frequencies. The intersection points of the curves shifts in the direction of increasing frequency due to the effects of temperature and neutron irradiation. This suggests that the rate of ionic polarization increases as a result of temperature and radiation. On the other hand, additional trace elements formed within the sample as a result of irradiation may also cause shifting. Jonscher's "universal dielectric response" are observed in the region of frequencies above the point of intersection. The sharp changes in numerical value of real and imaginary parts of dielectric permittivity were observed at high frequencies. Simultaneously, the real parts of dielectric permittivity are almost linear at these frequencies. Imaginary parts of dielectric permittivity are almost linear at high frequencies as in real parts. The effect of the neutron irradiation are obviously observed in the imaginary parts of dielectric permittivity in the frequency range of 0.5MHz – 2.5MHz. On the other hand, the numerical value of dielectric permittivity sharply decrease in the high frequency regions. The decrease in the numerical value of dielectric permittivity in proportion to the increase in frequency may be due to the activation of the electric field by the charge carriers. In general, there is an increase in the real and imaginary parts of the dielectric permittivity after irradiation. This increase can be attributed to the extra polarization of additional charge carriers formed within the sample as a result of the influence of neutron flux.

Simultaneously, the dielectric losses of the 3C-SiC nanocrystals were comparatively studied before and after neutron irradiation. The experiments were conducted in the range of 0,1Hz – 2.5MHz frequency and 100K-400K temperature (with 25K step). In general approach, an increase in the dielectric losses was obviously observed in both $f(\tan\delta) \sim f(f)$ and $f(\tan\delta) \sim f(T)$ dependencies after neutron irradiation. This increase is usually explained by neutron transmutation, dangling bonds, defects or the formation of additional charge carriers. The dielectric losses of the 3C-SiC nanocrystals are increased in the $f(\tan\delta) \sim f(f)$ dependence with increasing of the frequency and there are "deflection" states at the certain values of the frequency which explained in detail in this chapter. In the $f(\tan\delta) \sim$

$f(T)$ dependencies, there are observed of the increase in dielectric losses with increasing of the temperature due to the defects, orientation or dipole polarizations. Simultaneously, the frequency dependence of the losses decreases after a certain value of frequency. This can be attributed to the sharp decrease in polarization after corresponding frequencies. At the same time, the “bending” in the current dependence shifts in the direction of increasing frequency after neutron irradiation. This is probably due to the further polarization of additional charge carriers or trace elements as a result of the influence of neutron irradiation. On the other hand, there is a slight increase in the numerical value of dielectric losses after irradiation by neutrons. This can be explained by the defects formed in the sample during neutron irradiation. Formed defects decelerate the motion of charge carriers and as a result, the numerical value of the dielectric losses increases slightly. In addition, polarization of new carriers after irradiation with neutrons may also contribute to a partial increase of losses. On the other hand, the frequency dependence of dielectric losses at constant temperatures of 100K, 200K, 300K and 400K has been considered to observe changes in neutron irradiation at different times.

The decrease in the dielectric losses of about 350K temperature is clearly observed at low frequencies. This reduction in 3C-SiC nanocrystals may be due to the metal-semiconductor transition. Moreover, an increase in dielectric losses due to neutron irradiation was also observed in temperature dependence. Simultaneously, the metal-semiconductor transition slightly shifts in the direction of decreasing temperature after neutron irradiation. In general, the metal-semiconductor transition in these materials can be explained by neutron transmutations, dangling bonds, defects or formation of additional charge carriers. On the other hand, the effects of neutron flux are clearly observed in the $f(\tan\delta)\sim f(T)$ dependencies at different fixed frequencies.

On the other hand, the paramagnetic centers and their nature in the nanocrystalline 3C-SiC particles were comparatively studied before and after neutron irradiation. Electron Paramagnetic Resonance (EPR) spectroscopic analyzes were conducted in the

range of 0.05 - 0.55 T (500 - 5500 Gauss) magnetic field. The range of 0.3270 - 0.3370 T, which more paramagnetic centers are observed was additionally considered. The effect of the neutron irradiation on the concentration of new formed V_{Si}^- and V_C^+ isotopes vacancies was investigated. The number of the paramagnetic centers were calculated in the different values of g-factors corresponded to local states existed around 3300G of the external field. There have been proposed possible mechanisms that can be caused to the current increase in the number of the paramagnetic resonance after neutron irradiation. EPR spectra at selected intervals in the free electron region are presented in Figure 10. EPR spectra were considered at two different powers in order to verify the stability of existing signals and also to distinguish the free radicals and rapid relaxation states in the free electron region (Figure 10a and b).

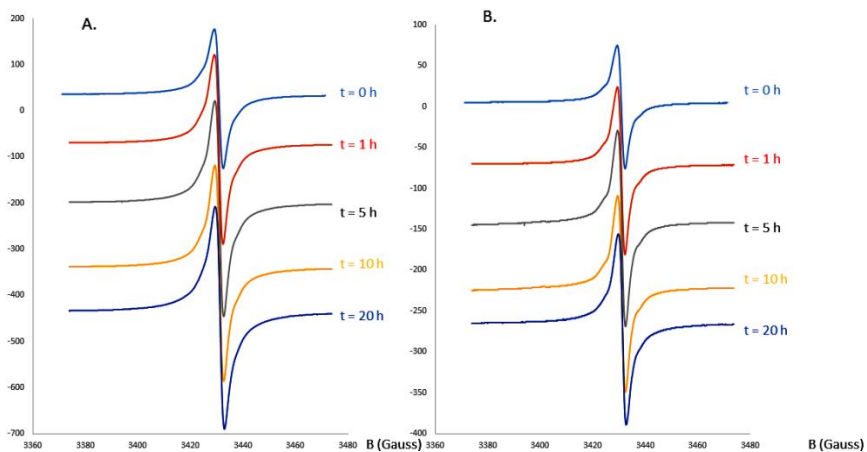


Figure 10. EPR spectra at different powers and selected intervals in the free electron region. (EPR parameters: central area 3320 G = 3.320 mT, sweep = 100G = 10 mT, modulation amplitude 0.1 mT, receiver rising 10, microwave power A. 20mW, B. 2mW).

It was defined from EPR analyzes performed at the saturation limit that existing signals are sufficiently stable. It was determined

that the existing signal observed on the 2.006 value of g factor is consist of two components (Table). One is a very strong signal which is observed at the 3300G and 20mW power, and at the 3030G and 2 mW power. The other is very broad and is not clearly visible from the spectra. It is clearly seen from the table that the number of free radicals increases in the general approach with the increase in the duration of neutron irradiation. As well as, about up to two times increase of the centers (2.006 value of g – factor) corresponded to free electrons are observed with increasing the irradiation duration. So that, the number of the centers corresponded to free electrons is 3.1×10^{16} center/cm³ (total number of the centers 4.5×10^{18} center/cm³) before irradiation, but this number is increased up to 5.7×10^{16} center/cm³ (total number of the centers 8.0×10^{18} center/cm³) after 20 hours irradiation.

Table. The number of the paramagnetic centers in the nanocrystalline 3C-SiC particles before and after neutron irradiation (N_0 and $N_{i.t.}$ are the number of the centers before and after irradiation (appropriate irradiation time), respectively).

During the irradiation by neutron flux (hours)	Numerical value of g – factor	Total centers ($N_{i.t.} - N_0$, c./cm ³)	g = 2.006 corresponded center ($N_{i.t.} - N_0$, c./cm ³)
0	2.29	0	0
	2.006		
1	2.13	1.5×10^{18}	0.7×10^{16}
	2.006		
5	2.58	1.6×10^{18}	1.5×10^{16}
	2.13		
10	2.006	3.3×10^{18}	2×10^{16}
	2.34		
20	2.006	3.5×10^{18}	2.7×10^{16}
	2.13		

In chapter VII, an influence of the neutron flux on the thermal properties of the nanocrystalline 3C-SiC particles have been considered. DSC (Differential Scanning Calorimetry), TGA (Thermogravimetric Analysis) and DTG (Differential Thermogravimetric Analysis) analyzes of the cubic modification nanocrystalline silicon carbide (3C-SiC) particles were performed depending on the thermal processing rate. The kinetical parameters (heat flux, oxidation reaction rate and activation energy) of the thermal effects formed with 5, 10, 15, and 25 K/min thermal processing rates in the range of 300 – 1270 K temperature were determined for silicon carbide nanoparticles with 99,5% purity. The activation energies of nanocrystalline 3C-SiC particles at different thermal processing rates were calculated using the Arrhenius approach. The oxidation rate of the nanocrystalline 3C-SiC particles has been studied up to 1270 K.

DSG and TG spectra of the nanocrystalline 3C-SiC particles at heating and cooling processes have been comparatively studied before and after neutron irradiation (Figure 11). As can be seen from the figure, there are additional traces that leave the environment in the DSC spectra up to about 800K temperatures (Figure 11a). However, there is no change in the TG spectrum, because the amount of the traces leaving the system is very small. At temperatures $T > 800\text{K}$, the stabilization of the DSC curves is observed.

Furthermore, there is observed an increase in the mass on the TG curves starting at $T > 900\text{K}$ of temperature. This process is usually explained by oxidation. This is confirmed in the cooling process. So that, almost no change in TG spectra is observed in the cooling process (Figure 11b). Neutron flux does not any characteristically changes in the DSC and TG spectra of 3C-SiC nanocrystal. However, neutron flux causes changes in the numerical value during the heat exchanges. Moreover, the oxidation process is relatively slow due to neutron flux (Figure 11a). This is probably due to the increase of the concentration of new more stable P isotopes as a result of the $^{31}\text{Si} \rightarrow (\beta\text{-decay}) ^{31}\text{P}$ nuclear transmutations.

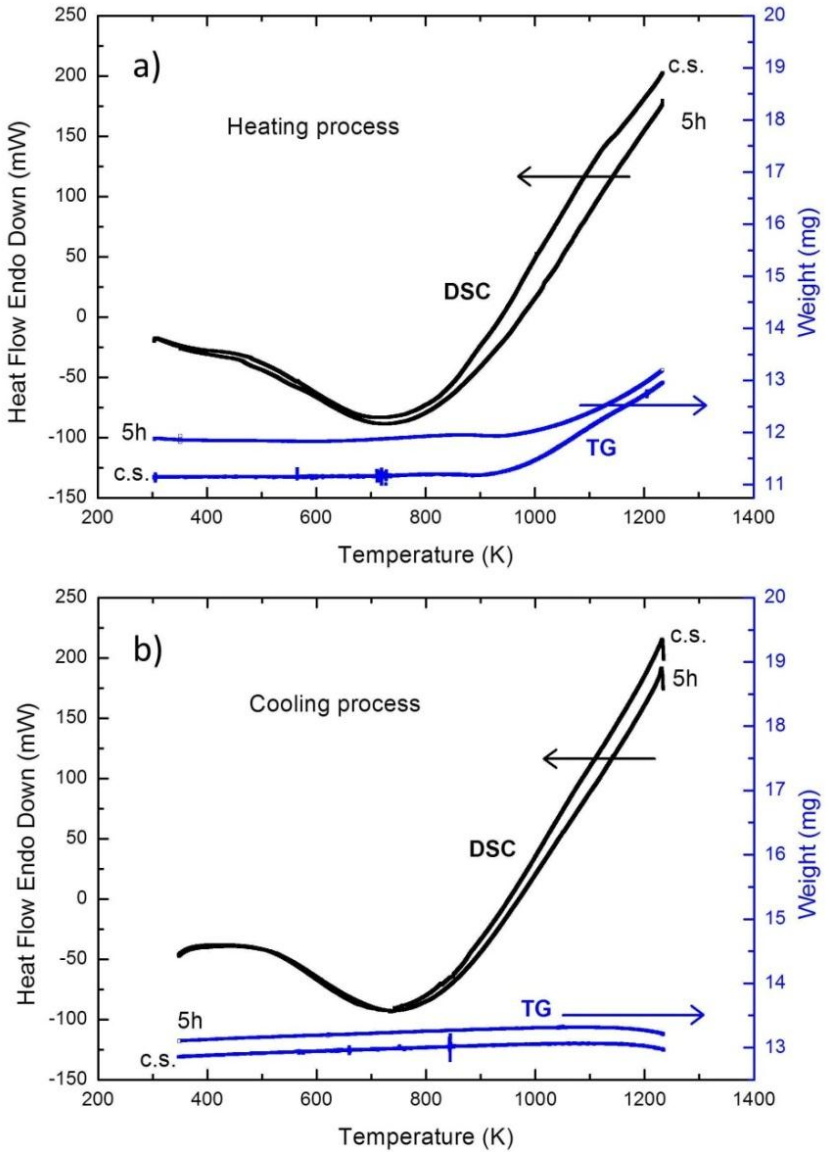


Figure 11. DSC and TG spectra (a heating process, b cooling process) of nanocrystalline 3C-SiC particles before (c.s.) and after (5h) neutron irradiation.

The temperature dependence of free Gibbs energy for 3C-SiC nanoparticles was calculated based on the experimental results. Free Gibbs energy was calculated separately before and after neutron irradiation, during the heating and cooling processes. The numerical value of the free Gibbs energy at relatively low temperatures is around 0 and sometimes gets negative values. Changing around zero of the numerical value of free Gibbs energy explains the equilibrium of the system. Moreover, the negative value of the free Gibbs energy is an indication that the processes occurring in the system are spontaneous and moving towards the equilibrium of the system. The numerical value of the free Gibbs energy is positive at the temperature of $T > 800\text{K}$ and in this case, the processes occurring in the system are not spontaneous.

The temperature dependencies of specific heat capacity of the nanocrystalline 3C-SiC particles in different thermal processing rates are given in Figure 12. There is a proportionality with the specific heat capacity and heating rate in the selected low temperature region (in the range of 300 K – 350 K temperature) (Figure 12a). However, the temperature dependence of the specific heat capacity is chaotic in the wide temperature range (300K - 1200K) of the temperature (Figure 12b). The numerical value of the specific heat capacity is around typical value for SiC ($750 \text{ C}\cdot\text{kg}^{-1}\text{K}^{-1}$) in the low temperature range. Nevertheless, there are sharp deviations with rising the temperature. The numerical value of the specific heat capacity is negative at about $T \geq 800\text{K}$ temperature. This is indicated that there are observed exothermic effects in the nanocrystalline 3C-SiC particles at $T \geq 800\text{K}$ temperatures. So that, the temperature of sample holder (pan) of the sample is less than the temperature of the sample. On the other hand, the numerical value of specific heat capacity is positive in the range of 300K-800K temperature or in general approach, corresponds to endothermic processes.

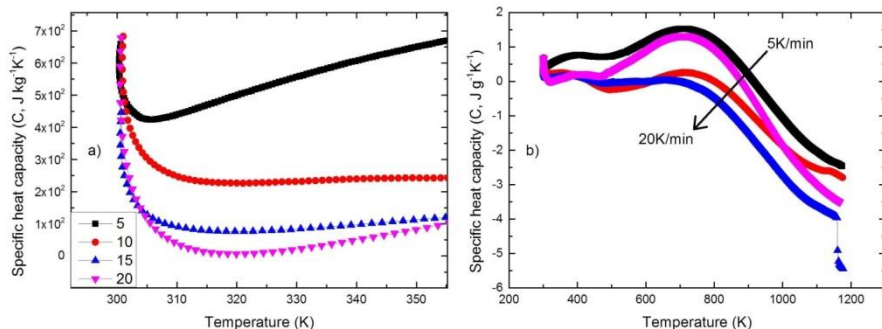


Figure 12. Temperature dependencies of specific heat capacity of the nanocrystalline 3C-SiC particles at different thermal processing rates (a selected range, b wide range).

The mass changes of nanocrystalline 3C-SiC particles depending on the temperature have been considered in detail at different thermal processing rate. It was determined that, very small changes in mass are observed with increasing temperature. There is a slight decrease in the temperature of $T < 800^{\circ}\text{C}$, which can be explained by the additional mixtures adsorbed within the sample. However, there is a slight increase in temperature, starting with the $T > 800^{\circ}\text{C}$ temperature. The cause may be oxidation, but more analytical work is needed to confirm this. The temperature dependence of oxidation rate was established using “Pyris Manager” software. It was found that the oxidation is very low in the nanocrystalline 3C-SiC particles up to 1270K temperature. There is almost no oxidation, in particular, at temperatures up to 1000K. Nevertheless, there is observed slight oxidation at temperatures more than 1000K and in general approach, the oxidation rate practically is close to zero. This proves that these materials are resistant to oxidation at high temperatures.

The temperature dependence of heat flux (DSC) of nanocrystalline 3C-SiC particles irradiated with neutron flux at different times has been explained. In the general approach, the influence of the neutron flux in the temperature dependence of heat flux is negligible and chaoticity is observed. Conducted experiments

show that the thermal processes carried out in the nanocrystalline 3C-SiC nanoparticles before and after neutron irradiation mainly can be explained with one part. Other minor deviations can be considered as the discharge of adsorbing water or other trace elements in the atmosphere from the system. So that, this step ends at about 400K of temperature. The main step continues about up to 800K of temperature. Nanomaterials have a huge specific surface area (SSA) and considered surfactants, therefore, in the general approach, it is assumed that the water or other compounds that become surface-dependent on contact with the atmosphere leave the nanoparticles at this step. This process continues up to about 800K of temperature.

The temperature given to the system in the temperature range $800 < T < 1300\text{K}$ is spending on the heating of the sample and no other effects are observed. However, the observation of analogical case in the cooling process in some sense, there is contradiction with the assumption that the system-dependent substances leave the system at 800 K temperature. This is usually explained by more or less the Debay temperature. However, unlike the case in the literature, the Debay temperature for silicon carbide is 1270K. In this case, it can be argued that the the Debay temperature decreases to 800K in the SiC nanoparticles under the influence of scale. The peak in the cooling process is probably related to trace elements that re-enter the system from the outside.

Moreover, the specific heat capacity and Gibbs energy of silicon carbide nanoparticles are determined at 5, 10, 15 and 25 K/min thermal processing rates in the range of 300 – 1270K temperature. The enthalpy and entropy of system composed of nanocrystalline 3C-SiC particles were calculated in different thermal processing rates (theoretical calculations are based on experimental results). Experimentally obtained results were comparatively studied in different thermal processing rates for all thermophysical parameters. Simultaneously, DSC, TGA and DTG analyzes were performed for the nanocrystalline silicon carbide (3C-SiC) particles irradiated by neutron flux (2×10^{13} n/cm²s) up to 5 hours at the TRIGA Mark II type nuclear research reactor. The oxidation rate of nanocrystalline 3C-SiC particles modified by neutron flux was

studied in the range $300\text{K} < T < 1300\text{K}$ temperature. Some effects were observed and explained in the TGA and DSC curves before and after neutron irradiation. It has been found that neutron flux causes changes in the numerical value of heat exchanges. Moreover, it has been shown that the oxidation process is relatively slow due to influence of the neutron flux. The typical ($500 \div 750 \text{ C} \cdot \text{kg}^{-1} \text{K}^{-1}$) value of the specific heat capacity was determined for 3C-SiC nanocrystals.

MAIN CONCLUSIONS

1. The existing atoms in the crystal lattice were observed at high magnification by HRTEM analyzes and nanocrystalline nature of the 3C-SiC particles were determined. It was revealed by HRTEM images that ~3nm amorphous layer is formed on the surface of nanocrystalline 3C-SiC particles at the high intensity (1.5×10^{18} neutron/cm²) of neutron irradiation. TEM and SEM analyzes revealed that agglomeration rarely exists in the nanocrystalline 3C-SiC particles at a maximum 70-80 nm range as a result of the influence of the neutron flux. 99.5+% purity of nanomaterial and the particular amount of trace elements existed in the material were determined by k_0 -INAA method.
2. The effective energy corresponded to maximum capture of neutron flux has been evaluated on the existing silicon and carbon isotopes in the 3C-SiC nanocrystals. The minimum energy of observed resonance states on the absorption spectra of the ²⁸Si, ²⁹Si and ³⁰Si isotopes are defined about $5 \cdot 10^{-2}$ MeV, 10^{-2} MeV and 10^{-3} MeV, respectively. It was shown that ³¹P isotope is formed as a result of the neutron capture in ³⁰Si isotope in the nanocrystalline 3C-SiC particles starting from 10^{-3} MeV of the energy of neutrons. The energies of the other (n, p), (n, α), (n, γ) and (n,n') transmutation for Si and C isotopes in the 3C-SiC nanocrystals were determined in the range of 3-7 MeV and 10-20 MeV, respectively.
3. It was found that it is possible to create donor dopants in the nanocrystalline 3C-SiC particles by neutron transmutation without any changes in the crystal structure. SAED, EDP and x-ray analyzes are shown that the structure of the 3C-SiC polytype does not change before and after neutron irradiation. Lattice parameters of 3C-SiC nanocrystals were defined as $a=b=c=4,377565$ and $\alpha=\beta=\gamma=90^0$.
4. RIC conductivity is observed as a result of the forms of n – type dopants in the nanocrystalline 3C-SiC under the influence of the neutron flux. The numerical value of the electrical conductivity of nanocrystalline 3C-SiC increases ~5.5 times as a result of the increase of formed dopant concentration. The numerical values of the calculated electrical activation energies decrease with increasing the

influence of duration of neutron flux (in other words dopant concentration) and frequency.

5. The resonance states were observed on the impedance spectra of nanocrystalline 3C-SiC particles modified by neutron flux and it was found that the relaxation times decrease from 3.5×10^{-2} second to 1.7×10^{-4} second. Semiconductor behaviour of the conductivity was determined from complex impedance spectroscopy of nanocrystalline 3C-SiC. Metal-semiconductor transitions occur in the 3C-SiC nanocrystals at $T_{MS} = 250K, 325K$ and $370K$ temperatures according to $0.1MHz, 1MHz$ and $2.5MHz$ of frequencies, respectively. In general approach, the metallic behaviour of nanocrystalline 3C-SiC were defined in the range of $f \geq 0.1MHz$ frequency and $T < T_{MS}$ temperature. It was established that the numerical value of T_{MS} decreases proportionally to the irradiation duration as a result of neutron transmutations, dangling bonds, formed defects or additional charge carriers.

6. The resistance of the nanocrystalline 3C-SiC reduced from $4 M\Omega$ to $1 M\Omega$ according to neutron doping. And it explained by the slop variation of linear Volt - Ampere characterization of nanocrystalline 3C-SiC. Fowler-Nordheim plots have shown that there is a direct tunnel junction and defined that thermal activity is dominant at all intervals in nanocrystalline 3C-SiC before and after irradiation.

7. It was discovered during the modification by neutron flux that the polarization of 3C-SiC nanoparticles on the intermediate surface cause to forms dispersion states. It was revealed that all observed dielectric dependencies corresponds to Havriliak–Negami phenological equations and ionic polarization is dominant.

8. The strong signal observed on the g value around 2.006 appropriate to the concentration of the n-type dopping element in the nanocrystalline 3C-SiC particles after the neutron irradiation. The current signals intensity increased and new signals appeared as a result of neutron irradiation rising duration. It has been found out additional ^{29}Si or ^{13}C isotopes in the nanocrystalline 3C-SiC by neutron irradiation. There were determined the anisotropic and

isotropic structure of Si (V_{Si}^-) and C (V_C^+) vacancies after neutron irradiation. The total number of new paramagnetic centers with vary g values revealed 3.5×10^{18} center/cm³ after neutron irradiation. The number of newly formed centers appropriate to free electrons (appropriate to 2.006 g-value) have been found out 2.7×10^{16} center/cm³ after neutron irradiation. It is important to note that, most of these centers are attributed to n-type doping elements.

9. The dielectric loss of nanocrystalline 3C-SiC decreasing throughout to frequency increasing. Moreover, on the $f(\tan\delta) \sim f(T)$ function it is clear that, dielectric loss is increasing in the course of temperature rise up. Simultaneously, from the $f(\tan\delta) \sim f(f)$ function, curving observed at the various value of frequency and slipping perceived accordingly to neutron irradiation. This situation thoroughly explains by the metal-semiconductor transition. The numerical value of the dielectric loss slightly increased in both $f(\tan\delta) \sim f(f)$ and $f(\tan\delta) \sim f(T)$ dependencies, after the neutron irradiation.

10. From the thermal investigation of nanocrystalline 3C-SiC, it found out that nanoparticles had very strong thermal stability up to 1270K before the neutron irradiation. Very slight oxidation observed in the $800K < T < 1270K$ intervals on the nanocrystalline 3C-SiC before neutron irradiation. However, the quantity of oxidation decreasing as a result of newly formed isotopes after neutron irradiation. Debye temperature of nanocrystalline 3C-SiC decreased from 1200K to 800K in consequence of particle size. From the DSC spectroscopy, before and after neutron irradiation the thermal activation energy and specific heat capacity of nanocrystalline 3C-SiC particles have been found out 120kJ/mol and $500 \div 750 J \cdot kg^{-1} K^{-1}$, respectively.

LIST OF PUBLICATION APPROPRIATE TO DISSERTATION RESULTS

1. Huseynov E., Anze J., Luka S. Temperature vs. impedance dependencies of neutron-irradiated nanocrystalline silicon carbide (3C-SiC) // *Applied Physics A*, 2019, v.125, pp.91-98
2. Huseynov E., Anze J. EPR spectroscopic studies of neutron-irradiated nanocrystalline silicon carbide (3C-SiC) // *Silicon*, 2019, v.11, pp. 21-27
3. Huseynov E.M. Current-voltage characteristics of neutron irradiated nanocrystalline silicon carbide (3CSiC) // *Physica B: Condensed Matter*, 2018, v.544, pp.23-27
4. Huseynov E.M. Electrical impedance spectroscopy of neutron-irradiated nanocrystalline silicon carbide (3C-SiC) // *Applied Physics A*, 2018, v.124, pp.191-198
5. Huseynov E.M. Neutron irradiation, amorphous transformation and agglomeration effects on the permittivity of nanocrystalline silicon carbide (3C-SiC) // *NANO*, 2018, v.13, No 3, pp.1830002
6. Huseynov E.M. Dielectric loss of neutron-irradiated nanocrystalline silicon carbide (3C-SiC) as a function of frequency and temperature // *Solid State Sciences*, 2018, v.84, pp.44-50
7. Huseynov E.M. Neutron irradiation effects on the temperature dependencies of electrical conductivity of silicon carbide (3C-SiC) nanoparticles // *Silicon*, 2018, v.10, pp.995–1001
8. Huseynov E.M. Neutron activation analysis of 3C-SiC nanoparticles under the neutron flux // *Journal of Radiation Researches*, 2018, v.5, No 1, pp.20-26
9. Hüseynov E.M. Nanokristallik silisium karbid (3C-SiC) hissəciklərində neytron zəbtinin tədqiqi // *Azerbaijan Journal of Physics*, 2018, v.24, No AZ1, pp.3-7
10. Hüseynov E.M. Neytron selinin təsiri ilə nanokristallik silisium karbid (3C-SiC) hissəciklərində (n , p) və (n , α) çevrilmələri // *AMEA – mın Xəbərləri, Fizika-texnika və riyaziyyat elmləri seriyası, fizika və astronomiya*, 2018, v.38, No 2, pp. 15-22
11. Hüseynov E.M., Əliyeva Ü.S., Mirzəyev M.N. Silisium karbid (3C-SiC) nanokristallarına neytron selinin təsirinin DSC spektroskopiyası ilə öyrənilməsi // *Bakı Universitetinin Xəbərləri, Fizika-riyaziyyat elmləri seriyası*, 2018, v.3, pp.161-170
12. Hüseynov E.M. Nanokristallik silisium karbid (3C-SiC)

hissəciklərində neytron selinin təsiri ilə defekt hallarının yaranması // Azerbaijan Journal of Physics, 2018, v.24, No AZ2, pp.3-10

13. Hüseynov E.M., Əliyeva Ü.S., Mirzəyev M.N. Neytron selinin təsiri altında nanokristallik silisium karbid (3C-SiC) hissəciklərinin DTA, TGA və DTG spektroskopik analizləri // AMEA – nın Xəbərləri, Fizika-texnika və riyaziyyat elmləri seriyası, fizika və astronomiya, 2018, v.38, No 5, pp. 65-71

14. Huseynov E., Anze J. Trace elements study of high purity nanocrystalline silicon carbide (3C-SiC) using k_0 -INAA method // Physica B: Condensed Matter, 2017, v.517, pp.30–34

15. Huseynov E.M. Permittivity-frequency dependencies study of neutron-irradiated nanocrystalline silicon carbide (3C-SiC) // NANO, 2017, v.12, No 6, pp.1750068

16. Huseynov E.M. Investigation of the agglomeration and amorphous transformation effects of neutron irradiation on the nanocrystalline silicon carbide (3C-SiC) using TEM and SEM methods // Physica B: Condensed Matter, 2017, v.510, pp.99–103

17. Huseynov E., Garibov A. Effects of neutron flux on the temperature dependencies of permittivity of 3C-SiC nanoparticles // Silicon, 2017, v.9, No 5, pp.753–759

18. Huseynov E.M. EDP study of nanocrystalline silicon carbide (3C-SiC) under the neutron irradiation // Journal of Radiation Researches, 2017, v.4, No 2, pp.24-30

19. Hüseynov E.M. Nanokristallik silisium karbid (3C-SiC) hissəciklərindən neytron selinin səpilməsi // Azerbaijan Journal of Physics, 2017, v.23, No AZ2, pp.24-32

20. Hüseynov E.M., Mirzəyev M.N. Nanokristallik silisium karbid (3C-SiC) hissəciklərinin termik parametrlərinin DSC metodu ilə tədqiqi // Bakı Universitetinin Xəbərləri, Fizika-riyaziyyat elmləri seriyası, 2017, v.4, pp.176-185

21. Hüseynov E.M., Mirzəyev M.N. DTA, TGA və DTG metodları ilə nanokristallik silisium karbid (3C-SiC) hissəciklərinin termofiziki parametrlərinin öyrənilməsi // AMEA – nın Xəbərləri, Fizika-texnika və riyaziyyat elmləri seriyası, fizika və astronomiya, 2017, v.37, No 5, pp.48-57

22. Huseynov E. Neutron irradiation and frequency effects on the electrical conductivity of nanocrystalline silicon carbide (3C-SiC) // Physics Letters A, 2016, v.380, pp.3086-3091

23. Hüseynov E.M., Qəribov A.A. TRIGA Mark II tipli tədqiqat nüvə

reaktorunda neytron selinin təsiri ilə 3C-SiC nanohissəciklərinin radioaktivlik tədqiqi // Azerbaijan Journal of Physics, 2016, v.22, No AZ3, pp.3-9

24. Huseynov E.M. Effects of neutron irradiation on the frequency dependencies of electrical conductivity of nanocrystalline 3C-SiC particles / DPG-Frühjahrstagung und EPS-CMD27, Technische Universität Berlin, Deutsche Physikalische Gesellschaft e.V., Berlin, Germany, 2018, p.137

25. Huseynov E.M. Impedance study of neutron-irradiated nanocrystalline silicon carbide (3C-SiC) as a function of temperature / 27th International Conference Nuclear Energy for New Europe, Slovenia, 2018, p.95-96

26. Huseynov E.M. Nanoscopic study of neutron irradiated nanocrystalline silicon carbide (3C-SiC) particles / 2nd International congress on semiconductor materials and devices, Turkey, 2018, p.120-121

27. Hüseynov E. Nanokristallik silisium karbid (3C-SiC) hissəciklərində neytronlarla şüalanma zamanı (n, p) və (n, α) çevrilmələrinin limit enerjiləri / Ümummilli lider Heydər Əliyevin anadan olmasının 95-ci ildönümünə həsr olunmuş Gənc Tədqiqatçıların II Beynəlxalq Elmi Konfransı, Bakı, 2018, s.67-69

28. Huseynov E.M. Frequency – electrical impedance dependencies of neutron irradiated nanocrystalline silicon carbide (3C-SiC) / XXVII International Materials Research Congress, F2. Advances in functional semiconducting materials - IMRC2018, Cancun, Mexico, 2018, p.2879-2880

29. Huseynov E.M. Neutron irradiation effects on the dielectric loss of nanocrystalline silicon carbide (3C-SiC) / VIII International Conference, Semipalatinsk Test Site: Legacy and Prospects for Scientific and Technical Potential Development, Kurchatov, Republic of Kazakhstan, 2018, p.161-162

30. Huseynov E.M. Permittivity vs. temperature dependencies of neutron irradiated nanocrystalline silicon carbide (3C-SiC) / XXI Simposio Chileno de Física Antofagasta, SOCHIFI, Area H: Materia Condensada Fis. Estado Solido, Chile, 2018, p.SPH04.1-2

31. Huseynov E.M. Temperature - electrical conductivity dependencies of silicon carbide (3C-SiC) nanoparticles exposed to neutron irradiation / International scientific conference of students and young scientists "Lomonosov-2018", Moscow, 2018, p. 34.14.1-3

32. Huseynov E.M. Neutron activation analysis of high purity nanocrystalline silicon carbide (3C-SiC) particles / 11th International

Conference «Nuclear and radiation physics» / Almaty, Republic of Kazakhstan, 2017, p.374

33. Huseynov E. Investigation of the Paramagnetic Centers of Neutron - Irradiated Nanocrystalline Silicon Carbide (3C-SiC) Particles / 26th International Conference Nuclear Energy for New Europe, Slovenia, 2017, p.55

34. Huseynov E. Frequency dependencies of electrical conductivity of silicon nanoparticles exposed to neutron flux / 25th International Conference Nuclear Energy for New Europe, Slovenia, 2016, p.42-43

35. Huseynov E.M. Investigation of thermal parameters of nanocrystalline silicon carbide (3C-SiC) particles using DSC method / I International scientific conference of young researchers, Baku Engineering University, Baku, 2017, p.39

A handwritten signature in blue ink, appearing to be 'Huseynov E.M.', is located in the lower right quadrant of the page.

The defense will be held on 07 May 2021 at 15⁰⁰ at the meeting of the Dissertation council BED 1.21 of Supreme Attestation Commission under the President of the Republic of Azerbaijan operating at the Institute of Radiation Problems of Azerbaijan National Academy of Sciences

Address: AZ1143, B.Vahabzadeh 9, Baku

Dissertation is accessible at the Institute of Radiation Problems of Azerbaijan National Academy of Sciences

Electronic versions of dissertation and its abstract are available on the official website of the Institute of Radiation Problems of Azerbaijan National Academy of Sciences

Abstract was sent to the required addresses on 02 April 2021

Signed for print: 19.03.2021

Paper format: A5

Volume: 75500 characters

Number of hard copies: 50